



# Bromine and iodine chemistry in a global chemistry-climate model: description and evaluation of very short-lived oceanic sources

C. Ordóñez<sup>1</sup>, J.-F. Lamarque<sup>2</sup>, S. Tilmes<sup>2</sup>, D. E. Kinnison<sup>2</sup>, E. L. Atlas<sup>3</sup>, D. R. Blake<sup>4</sup>, G. Sousa Santos<sup>5</sup>, G. Brasseur<sup>6</sup>, and A. Saiz-Lopez<sup>1</sup>

<sup>1</sup>Laboratory for Atmospheric and Climate Science (CIAC), CSIC, Toledo, Spain

<sup>2</sup>Atmospheric Chemistry Division, NCAR, Boulder, CO, USA

<sup>3</sup>University of Miami, Miami, FL, USA

<sup>4</sup>University of California, Irvine, CA, USA

<sup>5</sup>Institute of Atmospheric and Climate Science, ETH, Zurich, Switzerland

<sup>6</sup>Climate Service Center, Hamburg, Germany

Correspondence to: A. Saiz-Lopez (a.saiz-lopez@ciac.jccm-csic.es)

Received: 1 September 2011 – Published in Atmos. Chem. Phys. Discuss.: 6 October 2011

Revised: 9 January 2012 – Accepted: 22 January 2012 – Published: 7 February 2012

**Abstract.** The global chemistry-climate model CAM-Chem has been extended to incorporate an expanded bromine and iodine chemistry scheme that includes natural oceanic sources of very short-lived (VSL) halocarbons, gas-phase photochemistry and heterogeneous reactions on aerosols. Ocean emissions of five VSL bromocarbons ( $\text{CHBr}_3$ ,  $\text{CH}_2\text{Br}_2$ ,  $\text{CH}_2\text{BrCl}$ ,  $\text{CHBrCl}_2$ ,  $\text{CHBr}_2\text{Cl}$ ) and three VSL iodocarbons ( $\text{CH}_2\text{ICl}$ ,  $\text{CH}_2\text{IBr}$ ,  $\text{CH}_2\text{I}_2$ ) have been parameterised by a biogenic chlorophyll-*a* (*chl-a*) dependent source in the tropical oceans ( $20^\circ\text{N}$ – $20^\circ\text{S}$ ). Constant oceanic fluxes with 2.5 coast-to-ocean emission ratios are separately imposed on four different latitudinal bands in the extratropics ( $20^\circ$ – $50^\circ$  and above  $50^\circ$  in both hemispheres). Top-down emission estimates of bromocarbons have been derived using available measurements in the troposphere and lower stratosphere, while iodocarbons have been constrained with observations in the marine boundary layer (MBL). Emissions of  $\text{CH}_3\text{I}$  are based on a previous inventory and the longer lived  $\text{CH}_3\text{Br}$  is set to a surface mixing ratio boundary condition. The global oceanic emissions estimated for the most abundant VSL bromocarbons –  $533\text{ Gg yr}^{-1}$  for  $\text{CHBr}_3$  and  $67.3\text{ Gg yr}^{-1}$  for  $\text{CH}_2\text{Br}_2$  – are within the range of previous estimates. Overall the latitudinal and vertical distributions of modelled bromocarbons are in good agreement with observations. Nevertheless, we identify some issues such as the reduced number of aircraft observations to validate models in the Southern Hemisphere, the overestimation of  $\text{CH}_2\text{Br}_2$  in the upper troposphere – lower stratosphere and the underestimation of  $\text{CH}_3\text{I}$  in the same region. Despite the difficulties involved in the global modelling of the shortest lived iodocarbons ( $\text{CH}_2\text{ICl}$ ,  $\text{CH}_2\text{IBr}$ ,  $\text{CH}_2\text{I}_2$ ),

modelled results are in good agreement with published observations in the MBL. Finally, sensitivity simulations show that knowledge of the diurnal emission cycle for these species, in particular for  $\text{CH}_2\text{I}_2$ , is key to assess their global source strength.

## 1 Introduction

Combined reactive bromine and iodine species can alter the oxidative capacity of the troposphere through a number of processes. These include the depletion of ozone through efficient catalytic cycles (e.g. von Glasow and Crutzen, 2007; Saiz-Lopez et al., 2007; Read et al., 2008), the alteration of the partitioning of  $\text{HO}_x$  and  $\text{NO}_x$  (e.g. Bloss et al., 2005), the oxidation of dimethyl sulphide (DMS) (e.g. Boucher et al., 2003), and the conversion of elemental mercury ( $\text{Hg}^0$ ) to oxidized mercury ( $\text{Hg}^{\text{II}}$ ) (e.g. Schroeder et al., 1998; Calvert and Lindberg, 2003; Holmes et al., 2010; Obrist et al., 2011). Bromine compounds with a long enough tropospheric lifetime can also be transported to the stratosphere where they contribute to ozone depletion (e.g. WMO, 2007, 2011). While Solomon et al. (1994) speculated that iodine abundances of 1 pptv and/or fast rate constants for the chemistry coupling between iodine and bromine-chlorine could be of substantial importance to stratospheric ozone loss, the latest Scientific Assessments of Ozone Depletion (WMO, 2007, 2011) indicate that it is unlikely that iodinated gases are important for stratospheric ozone loss in the present day atmosphere.

Well known bromine sources include the long-lived anthropogenic halons, methyl bromide ( $\text{CH}_3\text{Br}$ ), very short-lived bromocarbons, and release from sea-salt aerosols. Halons are long-lived organic compounds containing bromine and other halogen atoms, primarily used as fire extinguishing agents; because of their long tropospheric lifetime they are transported to the stratosphere where they cause ozone depletion (e.g. Wamsley et al., 1998; Fraser et al., 1999; Schauffler et al., 1999). Very short-lived (VSL) halocarbons are defined as trace gases whose local lifetimes are comparable to, or shorter than, tropospheric transport timescales and that have non-uniform tropospheric abundances; in practice, they are considered to be compounds having atmospheric lifetimes of less than 6 months (WMO, 2007, 2011).  $\text{CH}_3\text{Br}$  is the most abundant brominated gas in the free troposphere and it has the longest tropospheric lifetime of all bromocarbons ( $\sim 0.7$  yr), excluding the halons (WMO, 2007). As a consequence,  $\text{CH}_3\text{Br}$  is one of the most important contributors to the bromine loading in the lower stratosphere (Schauffler et al., 1993; Kourtidis et al., 1998; Dvortsov et al., 1999).  $\text{CH}_3\text{Br}$  has sources of both natural and anthropogenic origin, including agricultural and industrial fumigation, combustion of leaded fuel, biomass burning, vegetation and terrestrial ecosystems, and oceanic production (Warwick et al., 2006b, and references therein). The most abundant brominated VSL species are predominantly of natural oceanic origin: bromoform ( $\text{CHBr}_3$ ), dibromomethane ( $\text{CH}_2\text{Br}_2$ ), bromochloromethane ( $\text{CH}_2\text{BrCl}$ ), bromodichloromethane ( $\text{CH}_2\text{BrCl}_2$ ), dibromochloromethane ( $\text{CHBr}_2\text{Cl}$ ). Identified sources for these compounds include macroalgae, ice algae and phytoplankton (e.g. Sturges et al., 1992; Carpenter and Liss, 2000; Quack and Wallace, 2003). Model studies (e.g. Dvortsov et al., 1999; Salawitch et al., 2005; Kerkweg et al., 2008; Brioude et al., 2010; Hossaini et al., 2010; Liang et al., 2010; Schofield et al., 2011) have highlighted the importance of bromocarbons for carrying bromine to the stratosphere. In addition to the photochemical destruction of bromocarbons, catalytic recycling on sea-salt aerosols also provides a source of bromine to the atmosphere (Vogt et al., 1996; Sander et al., 2003a). While sea-salt aerosol may be the main source of reactive bromine in the marine boundary layer (MBL) (Sander et al., 2003a), the photochemical breakdown of bromocarbons provides the main source of reactive bromine in the upper troposphere (Yang et al., 2005; Warwick et al., 2006a).

The oceans also provide the main source of iodine to the atmosphere through volatilisation of methyl iodide ( $\text{CH}_3\text{I}$ ) and the more reactive but less commonly reported dihalomethanes – chloriodomethane ( $\text{CH}_2\text{ICl}$ ), bromiodomethane ( $\text{CH}_2\text{IBr}$ ) and diiodomethane ( $\text{CH}_2\text{I}_2$ ). Since numerous field studies found no clear correlation between iodinated and brominated substances in either air or seawater, iodine compounds were thought to have a different marine source to their brominated analogues. As an example, Moore and Tokarczyk (1993) found higher bromocarbon

concentrations in coastal waters than in the pelagic zone, consistent with sources of those compounds from macroalgae, while  $\text{CH}_2\text{ICl}$  was elevated in surface open ocean waters, which can be interpreted as production by phytoplankton. However bromocarbons and iodocarbons are co-produced by many macrophytes and they have been repeatedly observed together at elevated concentrations (Carpenter et al., 1999, and references therein).  $\text{CH}_3\text{I}$  is likely to have both biological and non-biological sources in the ocean (e.g. Yokouchi et al., 2008). While there are indications of  $\text{CH}_3\text{I}$  production by macro- (Moore and Tokarczyk, 1993; Peters et al., 2005) and micro-algae (Moore et al., 1996), numerous studies point to photochemical production in the surface ocean rather than biological production as the dominant source (Moore and Zafriou, 1994; Happell and Wallace, 1996; Chuck et al., 2005; Yokouchi et al., 2008). Terrestrial sources including rice paddies, wetlands, biomass burning, and terrestrial biomes also contribute to the release of  $\text{CH}_3\text{I}$  to the atmosphere (Bell et al., 2002, and references therein). Other iodocarbons containing two or more halogen atoms (e.g. the above mentioned  $\text{CH}_2\text{I}_2$ ,  $\text{CH}_2\text{IBr}$ ,  $\text{CH}_2\text{ICl}$ ) have been reported in the MBL at much lower concentrations than  $\text{CH}_3\text{I}$  (e.g. Jones et al., 2010). These three species are referred to hereafter as  $\text{CH}_2\text{IX}$ . Because of the short lifetimes of iodinated compounds, ranging from a few days ( $\text{CH}_3\text{I}$ ) to a few minutes ( $\text{CH}_2\text{I}_2$ ), they are believed to be of importance mainly for the troposphere (WMO, 2011). However  $\text{CH}_3\text{I}$ , with a local lifetime of  $\sim 7$  days, can reach the tropical tropopause layer (TTL, defined as the layer with bottom at the region of maximum convective outflow at about 12 km altitude and upper end identical to the tropical cold point tropopause at about 17 km altitude) if emitted in the vicinity of deep convection cells (WMO, 2011).

A main difficulty for the modelling of bromine and iodine chemistry in the atmosphere is the description of the organic sources from halocarbons as well as the inorganic sources from sea-salt aerosols. Global emission magnitudes and distributions are not well constrained because of their high geographical and temporal variability. One of the first attempts to include both organic and inorganic bromine sources in a chemistry transport model (CTM) is that by Yang et al. (2005). Several emission scenarios of VSL bromocarbons are found in the literature. Among the most comprehensive studies focusing on their sources are those carried out by Warwick et al. (2006a), Kerkweg et al. (2008), and Liang et al. (2010). Warwick et al. (2006a) created a number of bromoform emission data sets, with different geographic distributions, to test flux predictions against atmospheric measurements and assess how well these observations constrain oceanic and coastal emissions. They scaled the emission fields of the other bromocarbons to the  $\text{CHBr}_3$  emission field. Liang et al. (2010) derived a “top-down” emission scenario – i.e. an emission inventory based on specified geographically distributed observed or estimated parameters such as measurements of background concentrations –

of  $\text{CHBr}_3$  and  $\text{CH}_2\text{Br}_2$  using observations from some NASA aircraft campaigns as constraints. Hossaini et al. (2010) developed a detailed chemical scheme for the degradation of these two source gases in a CTM to predict their distribution and that of their organic product gases. To our knowledge only Kerkweg et al. (2008) and Hossaini et al. (2012) have presented a detailed comparison of modelled profiles of other brominated VSL bromocarbons together with  $\text{CH}_3\text{Br}$  against aircraft measurements in the tropics. Some global modelling studies have simulated the atmospheric distribution of  $\text{CH}_3\text{I}$ , and used it as a tracer of marine convection (Bell et al., 2002) or evaluated its effects on stratospheric ozone (Brioude et al., 2010; Youn et al., 2010). The inclusion of iodine-containing dihalometanes ( $\text{CH}_2\text{IX}$ ) in global models is much more problematic because of the lack of observations and therefore the very limited knowledge on the magnitude and geographical location of their sources.

Here we present the first implementation of VSL oceanic sources and tropospheric chemistry of bromine and iodine in a chemistry-climate model. We have derived an emission inventory for very short-lived bromocarbons ( $\text{CHBr}_3$ ,  $\text{CH}_2\text{Br}_2$ ,  $\text{CH}_2\text{BrCl}$ ,  $\text{CHBrCl}_2$ ,  $\text{CHBr}_2\text{Cl}$ ) and iodocarbons ( $\text{CH}_2\text{ICl}$ ,  $\text{CH}_2\text{IBr}$ ,  $\text{CH}_2\text{I}_2$ ) using a compilation of aircraft campaigns and some observations available in the MBL, respectively.

## 2 General model description

CAM-Chem is the global three-dimensional Community Atmosphere Model (CAM) (Gent et al., 2010), modified to include interactive chemistry and calculate distributions of gases and aerosols. CAM-Chem has recently been used in a variety of applications (e.g. Lamarque et al., 2010, 2011; Lamarque and Solomon, 2010) in the same configuration as used here, i.e. with a horizontal resolution of  $1.9^\circ$  (latitude)  $\times$   $2.5^\circ$  (longitude) and 26 hybrid vertical levels from the surface to approximately 40 km, and a model timestep of 30 min. To successfully simulate the chemistry above 100 hPa, the model includes a representation of stratospheric chemistry (including polar ozone loss associated with stratospheric clouds) from the version 3 of MOZART (MOZART-3) (Kinnison et al., 2007) while the tropospheric chemistry mechanism is that of MOZART-4 (Emmons et al., 2010). For this study, we use a simplified tropospheric chemistry scheme with a prescribed monthly OH field taken from an integration for 2004 of a full chemistry version of MOZART-4 (Emmons et al., 2010). The global mean mass weighted OH concentration in the troposphere calculated for this OH field following Lawrence et al. (2001) is  $1.1 \times 10^6$  molecule  $\text{cm}^{-3}$  and yields an atmospheric methane lifetime of  $\sim 8.3$  yr. The scope of CAM-Chem has been extended to include natural sources of VSL halocarbons from the ocean; reactive chlorine, bromine and iodine species; related photochemical, gas-phase and heterogeneous reactions, as well as dry and wet deposition for relevant species (see details in Sect. 3).

In CAM-Chem, sulphate aerosol is formed by the oxidation of  $\text{SO}_2$  in the gas phase (by reaction with the hydroxyl radical) and in the aqueous phase (by reaction with ozone and hydrogen peroxide) (Tie et al., 2001, 2005). The model includes a representation of ammonium nitrate that is dependent on the amount of sulphate present in the air mass following a parameterisation of gas/aerosol partitioning (Metzger et al., 2002). Since only the bulk mass is calculated, a log-normal distribution is assumed for all aerosols using different mean radii and geometric standard deviations (Liao et al., 2003). We use a 1.6-day exponential lifetime for the conversion from hydrophobic to hydrophilic carbonaceous aerosols (organic and black). Mineral dust and sea salt aerosols are also implemented following Mahowald et al. (2006a, b), and the sources of these aerosols are derived based on the model-calculated wind speed and surface conditions.

At the lower boundary, the time-varying (monthly values) zonally-averaged distributions of  $\text{CO}_2$ ,  $\text{CH}_4$ ,  $\text{H}_2$ ,  $\text{N}_2\text{O}$  and all the long-lived halocarbons treated in the model (CFC-11, CFC-12, CFC-113, HCFC-22, H-1211, H-1301,  $\text{CCl}_4$ ,  $\text{CH}_3\text{CCl}_3$ ,  $\text{CH}_3\text{Cl}$  and  $\text{CH}_3\text{Br}$ ) are specified following their observed surface concentration for 2000. For the model simulations presented here, climatological sea surface temperatures and sea-ice extent (Rayner et al., 2003) are set as boundary conditions. Therefore, CAM-Chem only solves for the atmospheric and land portions of the climate system and the simulations do not pertain to any specific year. The model results shown here correspond to the last 1-yr simulation from a set of sequential simulations where VSL halocarbon emission sources were gradually optimised (see Sect. 4).

## 3 Chemistry of VSL halogen species in CAM-Chem

A comprehensive list of photochemical reactions and physical processes of the tropospheric halogen mechanism in CAM-Chem is shown in the Supplement. The mechanism follows that of the 1-dimensional Tropospheric HALOgen chemistry MOdel (THAMO) (Saiz-Lopez et al., 2008). In CAM-Chem, the five most abundant VSL bromocarbons ( $\text{CHBr}_3$ ,  $\text{CH}_2\text{Br}_2$ ,  $\text{CH}_2\text{BrCl}$ ,  $\text{CHBrCl}_2$ ,  $\text{CHBr}_2\text{Cl}$ ) and  $\text{CH}_3\text{I}$  are atmospherically processed via reaction with OH (see Table 1 in the Supplement) and photolysis (see Table 3 in the Supplement). The three shortest lived iodocarbons included in the model, i.e.  $\text{CH}_2\text{ICl}$ ,  $\text{CH}_2\text{IBr}$  and  $\text{CH}_2\text{I}_2$ , with lifetimes of hours to minutes, are only removed by photolysis. Similarly to most modelling studies we rely on the assumption that bromine from photo-oxidised VSL bromocarbons is immediately transformed to inorganic bromine. Model simulations with a detailed chemical scheme for the degradation of  $\text{CHBr}_3$  and  $\text{CH}_2\text{Br}_2$  indicate that such an assumption seems reasonable (Hossaini et al., 2010). The same applies to the photochemical breakdown of iodocarbons in CAM-Chem, with the exception of the removal of  $\text{CH}_3\text{I}$  by reaction with OH. This reaction yields the intermediate product  $\text{CH}_2\text{I}$ ,

which does not undergo further oxidation in the model; however this does not have a significant impact on the chemistry since this loss is negligible compared to photolysis. Rates of these and other reactions are calculated using temperature-dependent expressions from JPL 02-25 (Sander et al., 2003b) and JPL 06-02 (Sander et al., 2006) when available. To our knowledge there is not enough data for the reaction rates  $k$  ( $\text{CHBrCl}_2 + \text{OH}$ ) and  $k$  ( $\text{CHBr}_2\text{Cl} + \text{OH}$ ), and only estimates at 298 K ( $k_{298}$ ) are available for the first reaction (Bilde et al., 1998). For these two species we have adopted the activation energy of  $k$  ( $\text{CHBr}_3 + \text{OH}$ ) and scaled the  $A$  factor in the corresponding Arrhenius temperature-dependent expression to return the observed  $k_{298}$  ( $\text{CHBrCl}_2 + \text{OH}$ ) value. Photolysis rates of VSL halocarbons and other species are calculated using the absorption cross-sections and quantum yields reported in Atkinson et al. (2000, 2006) and Sander et al. (2006). Further detailed information on the tropospheric halogen chemistry scheme of CAM-Chem is given in the Supplement.

#### 4 Oceanic emissions of VSL halocarbons in CAM-Chem

##### 4.1 Background

A number of meridional surveys over the Atlantic and Pacific oceans have reported atmospheric concentrations of  $\text{CHBr}_3$  and other bromocarbons. Class and Ballschmiter (1988) revealed maximum concentrations of  $\text{CHBr}_3$  and to a lesser extent of  $\text{CH}_2\text{Br}_2$  and bromochloromethanes over the tropical East Atlantic near  $10^\circ\text{N}$ . Atlas et al. (1993) found a broad maximum of  $\text{CHBr}_3$  and  $\text{CH}_2\text{Br}_2$  near the equator where maximum chlorophyll was observed during a Pacific cruise. Similarly, air samples collected during the PEM-Tropics missions showed larger mixing ratios of  $\text{CHBr}_3$ ,  $\text{CH}_2\text{Br}_2$ ,  $\text{CHBr}_2\text{Cl}$  and  $\text{CHBrCl}_2$  in the tropics relative to mid-latitudes (Schauffler et al., 1993). These results point to significant marine biogenic sources of these species over the tropics. A review on bromoform's contribution to atmospheric chemistry showed that sea-air exchange is the main source for atmospheric bromoform, which is produced in the surface water by highly variable in space and time macroalgal sources and by planktonic organisms, while the anthropogenic bromoform sources due to water chlorination constitute a minor contribution of the global total emission (Quack and Wallace, 2003). They reported a number of studies that found correlation between chlorophyll-*a* (*chl-a*) and water bromoform in several open oceanic regions, while some studies in shelf areas did not yield such correlations possibly because the biotic correlation was masked by local anthropogenic contamination due to water chlorination. More recently, Carpenter et al. (2007) confirmed a widespread and productive source of  $\text{CHBr}_3$  in the northwest African coastal upwelling system between about  $10^\circ\text{N}$  and  $25^\circ\text{N}$ , and noted

a potential very strong source of tropical macroalgae. Elevated seawater and air concentrations of  $\text{CHBr}_3$  and  $\text{CH}_2\text{Br}_2$  were found in the high *chl-a* containing waters of that region, particularly for  $16^\circ\text{--}20^\circ\text{N}$ ,  $16^\circ\text{--}18^\circ\text{W}$  (Carpenter et al., 2009). Yamamoto et al. (2001) also observed depth profiles of iodocarbons ( $\text{CH}_2\text{I}_2$  and  $\text{CH}_2\text{ICl}$ ) very similar to those of *chl-a* in seawater collected from the Bay of Bengal under tropical stratified conditions, suggesting production by phytoplankton followed by rapid decay in seawater. The bromocarbons they observed ( $\text{CHBr}_3$  and  $\text{CH}_2\text{Br}_2$ ) were less localized in their distributions, suggesting a longer residence time in seawater after their release from phytoplankton.

Numerous studies have reported correlations among the atmospheric concentrations of VSL bromocarbons in the MBL at different locations over coastal areas and the open ocean, and interpreted them in terms of common marine sources (Carpenter et al., 1999, 2003, 2009; Carpenter and Liss, 2000; Yokouchi et al., 2005). As an example, Carpenter and Liss (2000) found that despite considerable variability in their concentrations, ratios of other bromocarbons to that of  $\text{CHBr}_3$  remained reasonably constant in different air masses, implying that the source emission ratios of these compounds are conserved over widespread regions. Yokouchi et al. (2005) found that the ratios of  $\text{CH}_2\text{Br}_2$  and  $\text{CHBr}_2\text{Cl}$  to bromoform showed a clear tendency to decrease with increasing  $\text{CHBr}_3$  concentration, which is consistent with emissions from macroalgae localised to coastal areas and with the fact that  $\text{CHBr}_3$  has the shortest lifetime among these compounds. Some of these analyses used background concentrations and ratios of bromocarbons, and assumed that they were globally representative to estimate their global emission rates (e.g. Yokouchi et al., 2005, and references therein; Carpenter et al., 2009, and references therein). Other model studies have estimated global emissions of bromocarbons based on top-down methods (e.g. Warwick et al., 2006a; Liang et al., 2010). They have assumed that bromocarbon emissions are highest in the tropics – e.g. between  $20^\circ\text{N}$  and  $20^\circ\text{S}$  in Scenario 5 of Warwick et al. (2006a) or between  $10^\circ\text{N}$  and  $10^\circ\text{S}$  in Liang et al. (2010) – significantly lower in the mid-latitudes (Warwick et al., 2006a; Liang et al., 2010), and null (Warwick et al., 2006a) or a small fraction of the total global amount (Liang et al., 2010) for latitudes over  $50^\circ$  in both hemispheres.

Progress has been made in understanding the sources of iodine to the atmosphere over the last few years, with a focus primarily on  $\text{CH}_3\text{I}$  and secondarily on  $\text{CH}_2\text{IX}$ . However, at present time there is no consensus on the origin, strength and geographical distribution of their sources. As discussed earlier, numerous studies point to photochemical production in the surface ocean as the dominant source of  $\text{CH}_3\text{I}$ . Bell et al. (2002) parameterised the marine production of  $\text{CH}_3\text{I}$  as a scaled product of the solar radiation flux at the surface and the dissolved organic carbon (DOC) concentration over the ocean. Based on estimates of macroalgal iodine sources to the atmosphere by Giese et al. (1999),

the 2002 Scientific Assessment of Ozone Depletion (WMO, 2003) suggested that polyhalogenated iodine compounds released from macroalgae ( $\text{CH}_2\text{ICl}$ ,  $\text{CH}_2\text{IBr}$ ,  $\text{CH}_2\text{I}_2$ ) make a very small contribution to the global iodine budget. However recent observations and 1-D model calculations by Jones et al. (2010) conclude that the combined ocean-to-atmosphere flux of these species provides a global iodine source comparable to that of  $\text{CH}_3\text{I}$ , and a surface iodine atom source 3–4 times higher due to their rapid photolysis rates. New laboratory data (Martino et al., 2009) also point to production of iodocarbons in seawater as the result of a purely chemical process depending on the presence of ozone, dissolved iodide, and dissolved organic matter (DOM). To our knowledge there have been no attempts to incorporate VSL iodine sources apart from those of  $\text{CH}_3\text{I}$  into global models.

#### 4.2 Implementation of VSL halogenated sources in CAM-Chem

We have implemented natural oceanic sources of halocarbons in CAM-Chem following previous reports on (i) the enhanced levels of bromocarbons over the tropics, (ii) the known biological sources of both bromocarbons and iodocarbons, (iii) the correlations found among some of these species, and (iv) their enhanced emissions over coastal areas. Our methodology is also based on that developed for bromocarbon emissions by previous model studies (e.g. Yang et al., 2005; Warwick et al., 2006a; Kerckweg et al., 2008; Sousa Santos, 2008; Liang et al., 2010). The halogenated VSL species included in CAM-Chem are five bromocarbons ( $\text{CHBr}_3$ ,  $\text{CH}_2\text{Br}_2$ ,  $\text{CH}_2\text{BrCl}$ ,  $\text{CHBrCl}_2$ ,  $\text{CHBr}_2\text{Cl}$ ), three iodine-containing dihalomethanes ( $\text{CH}_2\text{ICl}$ ,  $\text{CH}_2\text{IBr}$  and  $\text{CH}_2\text{I}_2$ ), and  $\text{CH}_3\text{I}$ . Note that  $\text{CH}_3\text{Br}$  is also considered here. To determine the emissions of bromocarbons and iodocarbons (except for  $\text{CH}_3\text{I}$  and  $\text{CH}_3\text{Br}$ ) we have used a compilation of measurements from a number of aircraft campaigns (see Table 1 and Fig. 1) and available observations in the MBL (see Table 2), respectively.

Following the work carried out by Sousa Santos (2008) to implement oceanic emissions of VSL bromocarbons in MOZART-4, we have correlated the production of bromoform to the biologically active areas in the tropical regions using a monthly climatology of *chl-a* provided by the SeaWiFS project for 1998–2003. These satellite data show a strong concentration enhancement in the tropical upwelling coastal regions that is related to efficient transport of nutrients to the surface waters and consequently to high primary production. The correlation between high productivity areas and primary halocarbon production is used to constrain bromoform emissions following the geographical distribution of the *chl-a* field in the latitude range from 20° N to 20° S. In the mid- and high-latitudes for both hemispheres (20°–50° and above 50°, respectively) we consider a constant oceanic flux for each of those four latitudinal bands as well as 2.5 higher emission fluxes over the coastal areas to account for

the stronger sources there compared to the open ocean. This 2.5 factor was found to yield a good fit between bromoform mixing ratios simulated by MOZART-4 and boundary layer measurements made during PEM-Tropics A and B (Sousa Santos, 2008). In the current version of CAM-Chem we do not attempt to represent the emissions associated with ice algae at the ice-water interface (Sturges et al., 1992, 1997), and therefore set emissions to null over the grid cells with ice fraction larger than zero.

We assume that the emission of bromoform and other VSL halocarbons is photosynthetically driven and depends on the actinic flux, with a diurnal variation described by a Gaussian profile peaking at noon and null at night. In our initial configuration, 70 % of the total  $\text{CHBr}_3$  flux was emitted in the tropics (20° S–20° N) following the *chl-a* field, while the non-chlorophyll-dependent emissions contributed to 25 % in the mid-latitudes (20°–50°), and the remaining 5 % in high latitudes (above 50°). This amounts to an initial annual global  $\text{CHBr}_3$  flux of  $\sim 480 \text{ Gg yr}^{-1}$ , value within the estimates given by Warwick et al. (2006a) and Liang et al. (2010) shown in Table 3. The geographical distribution of the remaining VSL bromocarbon emission fluxes is equivalent to that used for bromoform, as previously assumed by Warwick et al. (2006a). To derive the total emission sources we have initially applied the molar emission ratios of these species to bromoform according to previous literature reports and comparisons between collocated background observations (see details in Sousa Santos, 2008): 0.25 for  $\text{CH}_2\text{Br}_2$ , 0.04 for  $\text{CH}_2\text{BrCl}$ , 0.06 for  $\text{CHBr}_2\text{Cl}$  and 0.05 for  $\text{CHBrCl}_2$ . This approach can be summarised with the following formula:

$$E = 1.127 \times 10^5 \times f \times r \times \text{chl-}a \quad (1)$$

where

- $E$  = emission flux of a given species ( $\text{molecule cm}^{-2} \text{ s}^{-1}$ )
- $f$  = factor equal to 2 for  $\text{CHBr}_3$ , 0.50 for  $\text{CH}_2\text{Br}_2$ , 0.08 for  $\text{CH}_2\text{BrCl}$ , 0.12 for  $\text{CHBr}_2\text{Cl}$  and 0.10 for  $\text{CHBrCl}_2$ . Note that these are tentative values used so that our bromocarbon emission ratios coincide with those derived by Sousa Santos (2008). They were initially applied throughout the global oceans, but they were later modified separately for each species and latitudinal band during the iterative approach discussed below.
- $r$  = factor equal to 2.5 for coastal areas outside the tropics (i.e. model grid cells outside 20° S–20° N, with  $0 < \text{land.fraction} < 1$ ), and equal to 1 everywhere else over the global oceans and the tropical coastal areas.
- *chl-a* = chlorophyll-*a* 8-bit values (0–255) from a monthly climatology of SeaWiFS for the 1998–2003 period.

A 1-yr CAM-Chem simulation was conducted using these emission fluxes, taking initial conditions from the end of a

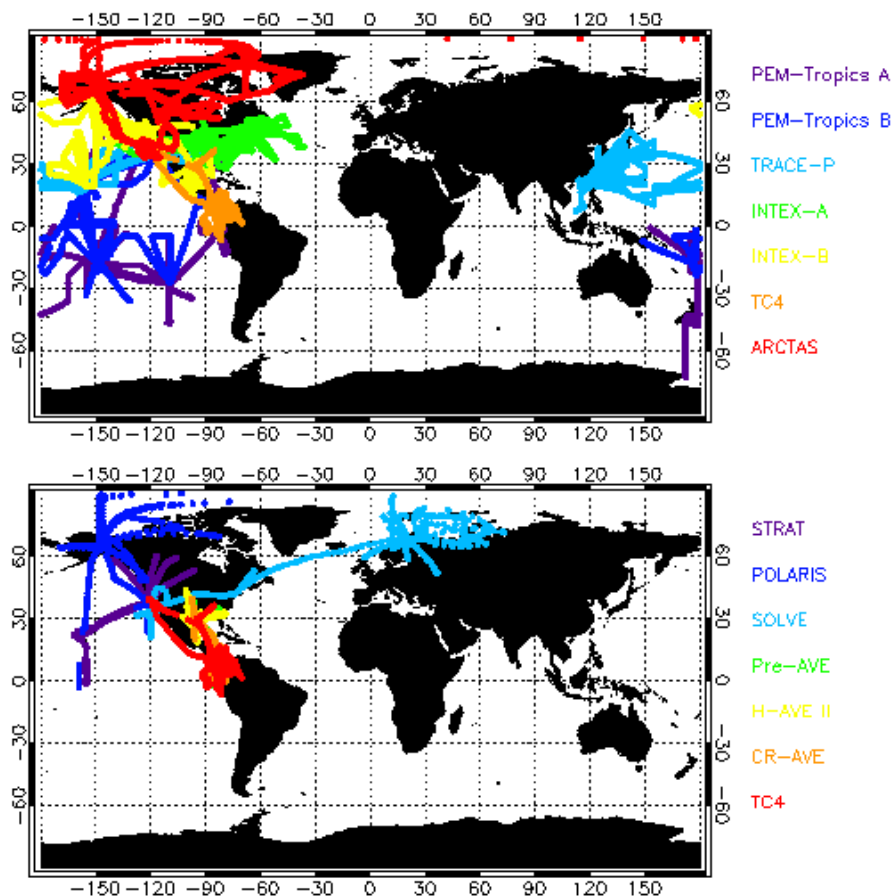


**Fig. 1.** Flight tracks of the aircraft campaigns analysed in this study. The upper and lower plots include the missions that have been used for the evaluation of halocarbon vertical profiles in the troposphere (1000–200 hPa) and the UTLS region (300–50 hPa), respectively. See more details in Table 1.

**Table 1.** Summary of the airborne observations used to estimate and evaluate VSL bromocarbon (i.e.  $\text{CHBr}_3$ ,  $\text{CH}_2\text{Br}_2$ ,  $\text{CH}_2\text{BrCl}$ ,  $\text{CHBrCl}_2$ ,  $\text{CHBr}_2\text{Cl}$ ) emissions in CAM-Chem.  $\text{CH}_3\text{Br}$  and  $\text{CH}_3\text{I}$  measurements were only used for the evaluation of these two species in the model. See flight tracks in Fig. 1.

Mission	Period	Species measured	Reference
PEM-Tropics A	Aug–Oct 1996	$\text{CHBr}_3$ , $\text{CH}_2\text{Br}_2$ , $\text{CHBrCl}_2$ , $\text{CHBr}_2\text{Cl}$ , $\text{CH}_3\text{Br}$ , $\text{CH}_3\text{I}$	Hoell et al. (1999)
PEM-Tropics B	Mar–Apr 1999	$\text{CHBr}_3$ , $\text{CH}_2\text{Br}_2$ , $\text{CHBrCl}_2$ , $\text{CHBr}_2\text{Cl}$ , $\text{CH}_2\text{BrCl}$ , $\text{CH}_3\text{Br}$ , $\text{CH}_3\text{I}$	Raper et al. (2001)
TRACE-P	Feb–Apr 2001	$\text{CHBr}_3$ , $\text{CH}_2\text{Br}_2$ , $\text{CHBrCl}_2$ , $\text{CHBr}_2\text{Cl}$ , $\text{CH}_2\text{BrCl}$ , $\text{CH}_3\text{Br}$ , $\text{CH}_3\text{I}$	Jacob et al. (2003)
INTEX-A	Jul–Aug 2004	$\text{CHBr}_3$ , $\text{CH}_2\text{Br}_2$ , $\text{CH}_3\text{Br}$ , $\text{CH}_3\text{I}$	Singh et al. (2006)
INTEX-B	Mar–May 2006	$\text{CHBr}_3$ , $\text{CH}_2\text{Br}_2$ , $\text{CH}_3\text{Br}$ , $\text{CH}_3\text{I}$	Singh et al. (2009)
TC4	Jul–Aug 2007	$\text{CHBr}_3$ , $\text{CH}_2\text{Br}_2$ , $\text{CHBrCl}_2$ , $\text{CHBr}_2\text{Cl}$ , $\text{CH}_2\text{BrCl}$ , $\text{CH}_3\text{Br}$ , $\text{CH}_3\text{I}$	Toon et al. (2010)
ARCTAS	Apr, Jun and Jul 2008	$\text{CHBr}_3$ , $\text{CH}_2\text{Br}_2$ , $\text{CH}_3\text{Br}$ , $\text{CH}_3\text{I}$	Jacob et al. (2010)
STRAT	Jan, Feb, Jul, Aug and Dec 1996	$\text{CHBr}_3$ , $\text{CH}_2\text{Br}_2$ , $\text{CHBr}_2\text{Cl}$ , $\text{CH}_3\text{Br}$	Schauffler et al. (1999)
POLARIS	Apr–Jul and Sep 1997	$\text{CHBr}_3$ , $\text{CH}_2\text{Br}_2$ , $\text{CHBrCl}_2$ , $\text{CH}_2\text{BrCl}$ , $\text{CH}_3\text{Br}$	Newman et al. (1999)
SOLVE	Dec 1999 and Jan–Mar 2000	$\text{CHBr}_3$ , $\text{CH}_2\text{Br}_2$ , $\text{CHBr}_2\text{Cl}$ , $\text{CH}_3\text{Br}$	Newman et al. (2002)
Pre-AVE	Jan–Feb 2004	$\text{CHBr}_3$ , $\text{CH}_2\text{Br}_2$ , $\text{CHBr}_2\text{Cl}$ , $\text{CH}_3\text{Br}$ , $\text{CH}_3\text{I}$	Hagan et al. (2004)
H-AVE II	Jun 2005	$\text{CHBr}_3$ , $\text{CH}_2\text{Br}_2$ , $\text{CHBr}_2\text{Cl}$ , $\text{CH}_3\text{Br}$ , $\text{CH}_3\text{I}$	Kroon et al. (2008)
CR-AVE	Jan–Feb 2006	$\text{CHBr}_3$ , $\text{CH}_2\text{Br}_2$ , $\text{CHBr}_2\text{Cl}$ , $\text{CH}_3\text{Br}$ , $\text{CH}_3\text{I}$	Kroon et al. (2008)

**Table 2.** Summary of the observations in the MBL used for the evaluation of iodine-containing dihalomethanes in CAM-Chem.

Location (latitude)	Type	Species	Reference
Southern ocean (49°–36° S)	Open ocean	CH <sub>2</sub> ICl	Chuck et al. (2005)
Cape Grim, Tasmania (41° S)	Coast (cliff top)	CH <sub>2</sub> ICl, CH <sub>2</sub> IBr, CH <sub>2</sub> I <sub>2</sub>	Carpenter et al. (2003)
Christmas Island (2° N)	Open ocean	CH <sub>2</sub> ICl	Varner et al. (2008)
Tropical/Subtropical East Atlantic (20° S–28° N)	Open ocean	CH <sub>2</sub> ICl	Chuck et al. (2005)
Hawaii (20° N)	Open ocean	CH <sub>2</sub> ICl	Varner et al. (2008)
Tropical East Atlantic (16°–23° N)	Upwelling	CH <sub>2</sub> ICl, CH <sub>2</sub> IBr, CH <sub>2</sub> I <sub>2</sub>	Jones et al. (2010), Lee et al. (2010)
Tropical East Atlantic (15°–25° N)	Open ocean	CH <sub>2</sub> ICl, CH <sub>2</sub> IBr, CH <sub>2</sub> I <sub>2</sub>	Jones et al. (2010), Lee et al. (2010)
Hateruma Island, Japan (24° N)	Open ocean	CH <sub>2</sub> ICl, CH <sub>2</sub> I <sub>2</sub>	Yokouchi et al. (2011)
Tropical East Atlantic (26°–36° N)	Open Ocean	CH <sub>2</sub> ICl, CH <sub>2</sub> IBr, CH <sub>2</sub> I <sub>2</sub>	Jones et al. (2010), Lee et al. (2010)
Thomson Farm, USA (43° N)	Coast	CH <sub>2</sub> ICl	Varner et al. (2008)
Cape Ochiishi, Japan (43° N)	Coast	CH <sub>2</sub> ICl, CH <sub>2</sub> I <sub>2</sub>	Yokouchi et al. (2011)
Roscoff, France (49° N)	Coast	CH <sub>2</sub> ICl, CH <sub>2</sub> IBr, CH <sub>2</sub> I <sub>2</sub>	Jones et al. (2009)
Mace Head, Ireland (53° N)	Coast	CH <sub>2</sub> ICl, CH <sub>2</sub> IBr, CH <sub>2</sub> I <sub>2</sub>	Carpenter et al. (1999, 2003)
Norfolk, England (53° N)	Coast	CH <sub>2</sub> ICl	Baker et al. (2001)
Dagebüll, North Sea (55° N)	Coast	CH <sub>2</sub> ICl, CH <sub>2</sub> IBr	Peters et al. (2005)
North East Atlantic (55°–57° N)	Shelf	CH <sub>2</sub> ICl, CH <sub>2</sub> IBr, CH <sub>2</sub> I <sub>2</sub>	Jones et al. (2010)

**Table 3.** Global annual fluxes and global annual average photochemical lifetime of VSL halogenated source gases of oceanic origin.

Source gas	Global annual flux (Gg yr <sup>-1</sup> )		Lifetime (this study)
	This study	Literature	
CHBr <sub>3</sub>	533	400 <sup>a</sup> , 595 <sup>b</sup> , 448 <sup>d</sup>	17 days
CH <sub>2</sub> Br <sub>2</sub>	67.3	113 <sup>c</sup> , 62 <sup>d</sup>	130 days
CH <sub>2</sub> BrCl	10.0	6.8 <sup>c</sup>	145 days
CHBr <sub>2</sub> Cl	19.7	23 <sup>c</sup>	56 days
CHBrCl <sub>2</sub>	22.6	16 <sup>c</sup>	46 days
CH <sub>3</sub> Br*	climatology	131 <sup>c</sup>	1.6 yr <sup>g</sup>
CH <sub>3</sub> I**	303	304 <sup>e</sup>	5 days
CH <sub>2</sub> ICl	234	236 <sup>f</sup>	8 h
CH <sub>2</sub> IBr	87.3	87 <sup>f</sup>	2.5 h
CH <sub>2</sub> I <sub>2</sub>	116	116 <sup>f</sup>	7 min

\* CH<sub>3</sub>Br has been included here for completeness. However it cannot be considered as VSL or of only oceanic origin, since its lifetime is longer than 6 months and it has some non-oceanic sources. The ocean is both a sink and a source for this gas.

\*\* The emission of CH<sub>3</sub>I in CAM-Chem comes from the inventory of Bell et al. (2002), which includes both oceanic and terrestrial fluxes.

<sup>a</sup> Scenario A from Warwick et al. (2006a). Also used in Yang et al. (2005).

<sup>b</sup> Scenario B from Warwick et al. (2006a). Also used in Kerkweg et al. (2008).

<sup>c</sup> Scenario A and B from Warwick et al. (2006a). Also used in Yang et al. (2005) and Kerkweg et al. (2008).

<sup>d</sup> Top-down estimate of Liang et al. (2010), referred to as Scenario A in that paper.

<sup>e</sup> Bell et al. (2002).

<sup>f</sup> Fluxes estimated from air and sea water measurements and 1-D atmospheric modelling (Jones et al., 2010).

<sup>g</sup> Atmospheric lifetime due to photochemical reactions. It does not include additional sinks such as ocean and soil uptake, which would reduce it to around 0.7 yr.

6-yr CAM-Chem simulation that already included VSL halogenated sources.

Following a top-down approach similar to that of Liang et al. (2010), we have carried out a set of sequential 1-yr model simulations and compared modelled bromocarbon mixing ratios with aircraft observations mainly within the troposphere (see Fig. 1, top) to gradually optimise the emission ratios assumed for these species over each of the five latitudinal bands. Note that only during PEM-Tropics A and B there were some flights south of 30° S, and not all with measurements for the different VSL species of interest. In order to extend the coverage of observations, we have also included surface observations for the two most abundant VSL bromocarbons, i.e. CHBr<sub>3</sub> and CH<sub>2</sub>Br<sub>2</sub>. We use published mixing ratios of CHBr<sub>3</sub> over open oceans prior to 2003 from Quack and Wallace (2003). We also include NOAA/CMDL cruise measurements of CH<sub>2</sub>Br<sub>2</sub> from 1994 to 2004 from the following missions: BLAST I (January–February 1994, Eastern Pacific), BLAST II (October–November 1994, Atlantic), BLAST III (February–April 1996, Antarctic), GasEx (May–July 1998, North Eastern Pacific and North Atlantic), BACPAC (September–October 1999, North Pacific), CLIVAR (November–December 2001, Southern oceans) and PHASE I (June–July 2004, North Pacific) (data available at: <ftp://ftp.cmdl.noaa.gov/hats/ocean/Ocean%20GCMS%20Data%201994-2004/>; Butler et al., 2007). These surface observations of CHBr<sub>3</sub> and CH<sub>2</sub>Br<sub>2</sub> were mainly used to improve our flux estimates in the southern mid and high-latitudes. Each iterative simulation starts with initial conditions from the end of the previous one. A number of simulations were needed to obtain a reasonably good agreement between modelled and observed atmospheric mixing ratios in order to derive the total emission fluxes as well as to ensure that all VSL halocarbons reached steady state.

As an example, Fig. 2 illustrates the resulting global distribution of the  $\text{CHBr}_3$  emission flux in July. The final global totals estimated following this approach are reported in Table 3 together with those from previous model studies. Our global estimate for  $\text{CHBr}_3$  ( $533 \text{ Gg yr}^{-1}$ ) is within the range estimated by other global models ( $400\text{--}595 \text{ Gg yr}^{-1}$ ), while our estimate for  $\text{CH}_2\text{Br}_2$  ( $67.3 \text{ Gg yr}^{-1}$ ) is considerably smaller than the  $113 \text{ Gg yr}^{-1}$  estimated by Warwick et al. (2006a) and slightly higher than the more recent value of  $62 \text{ Gg yr}^{-1}$  reported by Liang et al. (2010). There are more discrepancies in the emission estimates for the least abundant bromocarbons treated here ( $\text{CH}_2\text{BrCl}$ ,  $\text{CHBr}_2\text{Cl}$ ,  $\text{CHBrCl}_2$ ), most probably because of the uncertainties arising from the lack of measurements for these species; however the emission estimates are within 30 % agreement with other reported estimates. Note that the combined mass emission flux of  $\text{CHBr}_3$  and  $\text{CH}_2\text{Br}_2$  contributes more than 90 % to the total VSL bromocarbon flux. The global Br mass flux from VSL halocarbons in CAM-Chem ( $600 \text{ Gg Br yr}^{-1}$ ) is comparable to previous model estimates of  $513 \text{ Gg Br yr}^{-1}$  (Yang et al., 2005; Scenario A of Warwick et al., 2006a) and  $698 \text{ Gg Br yr}^{-1}$  (Scenario B of Warwick et al., 2006a; Kerkweg et al., 2008).

Regarding the geographical emission distribution, the percentages of  $\text{CHBr}_3$  and  $\text{CH}_2\text{Br}_2$  emitted for each latitudinal band are shown in Table 4. The contribution of  $\text{CHBr}_3$  emissions in the northern mid- and high latitudes is higher than that within the corresponding latitude bands in the Southern Hemisphere (SH). Although a similar result was previously found by Liang et al. (2010) (see their Table 1), there is no clear explanation for the higher fluxes in the Northern Hemisphere (NH) apart from the larger extent of coastal areas there. The inter-hemispheric differences found by this top-down analysis for  $\text{CH}_2\text{Br}_2$  emission fluxes are even larger, with fluxes in the NH doubling those in the SH. It is possible that these estimates are too low in the SH as a consequence of the lack of aircraft observations there. The use of the rather sparse surface observations of  $\text{CHBr}_3$  and  $\text{CH}_2\text{Br}_2$  in the flux calculation only yields a slight increase in the emission fluxes initially estimated from aircraft observations over the SH. This will be further discussed in Sect. 5.1.

To derive the total emission fluxes for  $\text{CH}_2\text{ICl}$ ,  $\text{CH}_2\text{IBr}$  and  $\text{CH}_2\text{I}_2$ , we followed a similar approach to that of the VSL bromocarbons, i.e. the  $\text{CH}_2\text{IX}$  emission fluxes consist of a chlorophyll-based source in the tropics ( $20^\circ \text{ N--}20^\circ \text{ S}$ ) as well as constant oceanic fluxes with a coast-to-ocean emission ratio of 2.5 for each of the other four latitudinal bands. The initial ratios to the chl-*a* field were set to match the global totals of Jones et al. (2010), which amount to  $\sim 440 \text{ Gg yr}^{-1}$  of  $\text{CH}_2\text{IX}$  (see Table 3). This results in *f* factors in Eq. (1) of 1.41 for  $\text{CH}_2\text{ICl}$ , 0.42 for  $\text{CH}_2\text{IBr}$  and 0.46 for  $\text{CH}_2\text{I}_2$ . With the iterative 1-yr model simulations conducted to optimise bromocarbon emissions we have also tested the impact of the diurnal profile of emissions and the coast-to-ocean emission ratio on the  $\text{CH}_2\text{IX}$  flux strength. The modelled

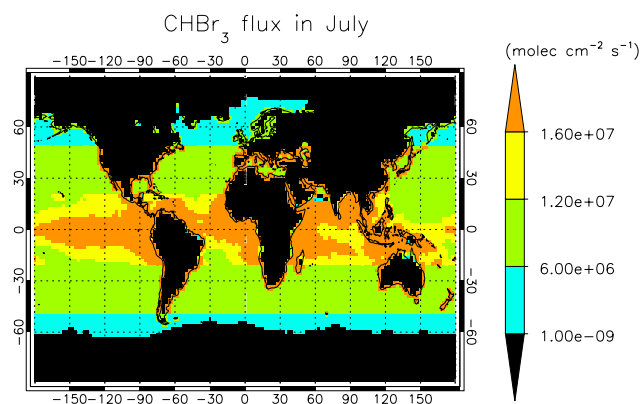


Fig. 2. Global emission distribution of  $\text{CHBr}_3$  estimated for July.

$\text{CH}_2\text{IX}$  mixing ratios were compared with surface observations available in the literature (see Table 2). However the very limited number of measurements available for these species makes it difficult to determine the magnitude and distribution of the iodine sources. A configuration with global totals matching those of Jones et al. (2010), a latitudinal distribution with strong sources in the tropics gradually decreasing towards the high-latitudes ( $\sim 66\%$  of the total flux within  $20^\circ \text{ N--}20^\circ \text{ S}$ ,  $15\%$  for  $20^\circ\text{--}50^\circ \text{ N}$ ,  $15\%$  for  $20^\circ\text{--}50^\circ \text{ S}$ , and  $4\%$  above  $50^\circ$ ), a coast-to-ocean emission ratio of 2.5 outside the tropics, and a Gaussian diurnal emission profile is finally used. The global totals of the  $\text{CH}_2\text{IX}$  emission fluxes are indicated in Table 3. Results from the comparison between observations and modelled fields are presented in Sect. 5.3, which also includes some analyses of the diurnal cycle of emissions.

The emissions of  $\text{CH}_3\text{I}$  in CAM-Chem are taken from the emission inventory of Bell et al. (2002). They include a major oceanic source ( $213 \text{ Gg yr}^{-1}$ ) as well as some land-based sources that may be regionally important.  $\text{CH}_3\text{I}$  fluxes from rice paddies ( $71 \text{ Gg yr}^{-1}$ ) are stronger than the other land-based sources – wetlands, biofuel and biomass burning – which amount to around  $20 \text{ Gg yr}^{-1}$ , yielding a global  $\text{CH}_3\text{I}$  flux of  $304 \text{ Gg yr}^{-1}$ .  $\text{CH}_3\text{Br}$  has a sufficiently long lifetime to be well-mixed in the troposphere and we impose a surface air concentration of 9 ppt based on observations for 2000. Available aircraft measurements of  $\text{CH}_3\text{I}$  and  $\text{CH}_3\text{Br}$  are also used to evaluate the atmospheric mixing ratios of these two species in CAM-Chem.

The global annually integrated atmospheric lifetimes due to photochemical loss for the halocarbon species considered here are reported in Table 3. The atmospheric lifetime of a given halocarbon is calculated as the ratio of its global atmospheric burden to the total removal rate from the atmosphere by photolysis and reaction with OH as simulated by CAM-Chem. Overall, the lifetimes of the most abundant VLS bromocarbons ( $\text{CHBr}_3$ ,  $\text{CH}_2\text{Br}_2$ ) and iodocarbons ( $\text{CH}_3\text{I}$ ) simulated by CAM-Chem are in good agreement with recent literature estimates, though in some cases close to the lower

**Table 4.** Emission distribution of  $\text{CHBr}_3$  and  $\text{CH}_2\text{Br}_2$  in CAM-Chem.

	Emission distribution (%)	
	$\text{CHBr}_3$	$\text{CH}_2\text{Br}_2$
50°–90° N	2.8	2.6
20°–50° N	22.5	22.1
20° N–20° S	55.6	63.1
20°–50° S	17.6	10.6
50°–90° S	1.5	1.6

limits: 17 days for  $\text{CHBr}_3$  compared to 20 days in Kerkweg et al. (2008) and Liang et al. (2010), and 15–37 days depending on the geographical distribution of emissions in Warwick et al. (2006a); 130 days for  $\text{CH}_2\text{Br}_2$  compared to 100 days in Kerkweg et al. (2008) and 140 days in Liang et al. (2010), and 5 days for  $\text{CH}_3\text{I}$ , somewhat shorter than the 6 days reported in Bell et al. (2002) and less than half the value (11 days) calculated in Youn et al. (2010). The lifetime reported here for  $\text{CH}_3\text{Br}$  (1.6 yr) is in line with previous estimates inferred from measurements (e.g. 1.7 yr in Yvon-Lewis and Butler, 1997, and references therein) and is also within the 1.5–1.8 yr (depending on the meteorological fields) simulated by Kinnison et al. (2007); note that this lifetime does not include additional sinks (e.g. ocean and soil uptake), which would reduce it to around 0.7 yr as estimated by Warwick et al. (2006b).  $\text{CHBr}_3$  and  $\text{CH}_3\text{I}$  are removed mostly by photolysis; reaction with OH controls the lifetimes of  $\text{CH}_2\text{Br}_2$  and  $\text{CH}_3\text{Br}$  in the troposphere, while both loss terms are comparable to each other in the stratosphere.

## 5 Comparison with observations and discussion

In this section the simulated bromocarbons and  $\text{CH}_3\text{I}$  mixing ratios are compared with a composite of atmospheric observations from a number of aircraft campaigns. Additional surface data are also employed for comparison with modelled  $\text{CHBr}_3$  and  $\text{CH}_2\text{Br}_2$ . The simulated  $\text{CH}_2\text{IX}$  mixing ratios are evaluated with published observations in the MBL.

### 5.1 Latitudinal distribution of bromocarbons

We compare modelled and observed bromocarbon mixing ratios within the following tropospheric layers: 1000–800 hPa, 800–600 hPa and 600–400 hPa. Note that the number of available measurements tends to be somewhat higher for 600–400 hPa than for 1000–800 hPa. This comparison was done on a monthly and seasonal basis, merging observations for the same month or season from aircraft campaigns that took place on different years. As a consequence, a 1-yr simulation cannot account for year-to-year variability in the atmospheric mixing ratios of halocarbons caused by differences in physical processes (e.g. convection, mixing of MBL

air, horizontal advection, solar irradiance) or the influence of various natural and even anthropogenic sources during each campaign. In the following, for all analyses shown here, modelled fields are sampled at the same locations and during the same months as the observations. As an example, Figs. 3 and 4 show seasonal composites for  $\text{CHBr}_3$  and  $\text{CH}_2\text{Br}_2$  in the boreal spring and summer within 1000–800 hPa as well as scatter-plots of modelled vs. observed fields for the three tropospheric layers mentioned above. Correlations between model and observations are generally higher for well-mixed air masses in the mid- to upper troposphere compared to those in the lower troposphere as well as for the relatively long-lived  $\text{CH}_2\text{Br}_2$  compared to  $\text{CHBr}_3$ , which is more affected by local sources. Such sources are evident from the underestimation of some observations in the model, in particular during summer when the aircraft flew over the North American continent as well as in a region over the Gulf of Mexico, and the tropical Eastern Pacific in the case of  $\text{CH}_2\text{Br}_2$ . With the exception of  $\text{CHBr}_3$  during summer, most data points fall within the 1:2 and 2:1 lines. Despite the reasonably good agreement between observations and model, note the limited observational data sets, with a lack of airborne measurements over the Atlantic and Indian oceans, in the southern extratropics, and during the boreal autumn and winter. In particular, observations for latitudes between 40° S and 90° S are very sparse, and they were collected during the boreal autumn (not shown). Thus, for the estimation of VSL halocarbon emission fluxes, there is not enough data to correct for the effect of seasonality over some areas.

Figure 5 illustrates the latitudinal distribution of modelled and observed bromocarbons for two tropospheric layers arbitrarily chosen to reflect the lower (1000–800 hPa) and mid-troposphere (600–400 hPa). The latitudinal distributions of  $\text{CHBr}_3$  and  $\text{CH}_2\text{Br}_2$  are generally well captured by the model, with elevated mixing ratios in the tropics and at high latitudes resulting from the enhanced emissions and the longer lifetime of these species in those regions, respectively. Observations of bromocarbons generally indicate higher mixing ratios for 0°–20° N compared to 0°–20° S, while the chl-*a* parameterisation used here tends to overestimate them over 0°–20° S. For example,  $\text{CHBr}_3$  is over-predicted by ~18 % within 1000–800 hPa and by less than 4 % within 600–400 hPa for this latitudinal range. The model also seems to overestimate the aircraft observations of  $\text{CHBr}_3$  for 20°–50° S by 25–30 %, although note again the reduced number of observations for those latitudes. The inclusion of surface observations over open ocean from Quack and Wallace (2003), with a larger number of observational points in the SH, results in a contribution to the total global flux of 17.6 % for 20°–50° S, compared to the 22.5 % estimated for 20°–50° N (Table 4). Figure 6 shows that the  $\text{CHBr}_3$  field from CAM-Chem, zonally averaged over the ocean and therefore not exactly collocated with observations, agrees reasonably well with the measurements considering their range of variability.

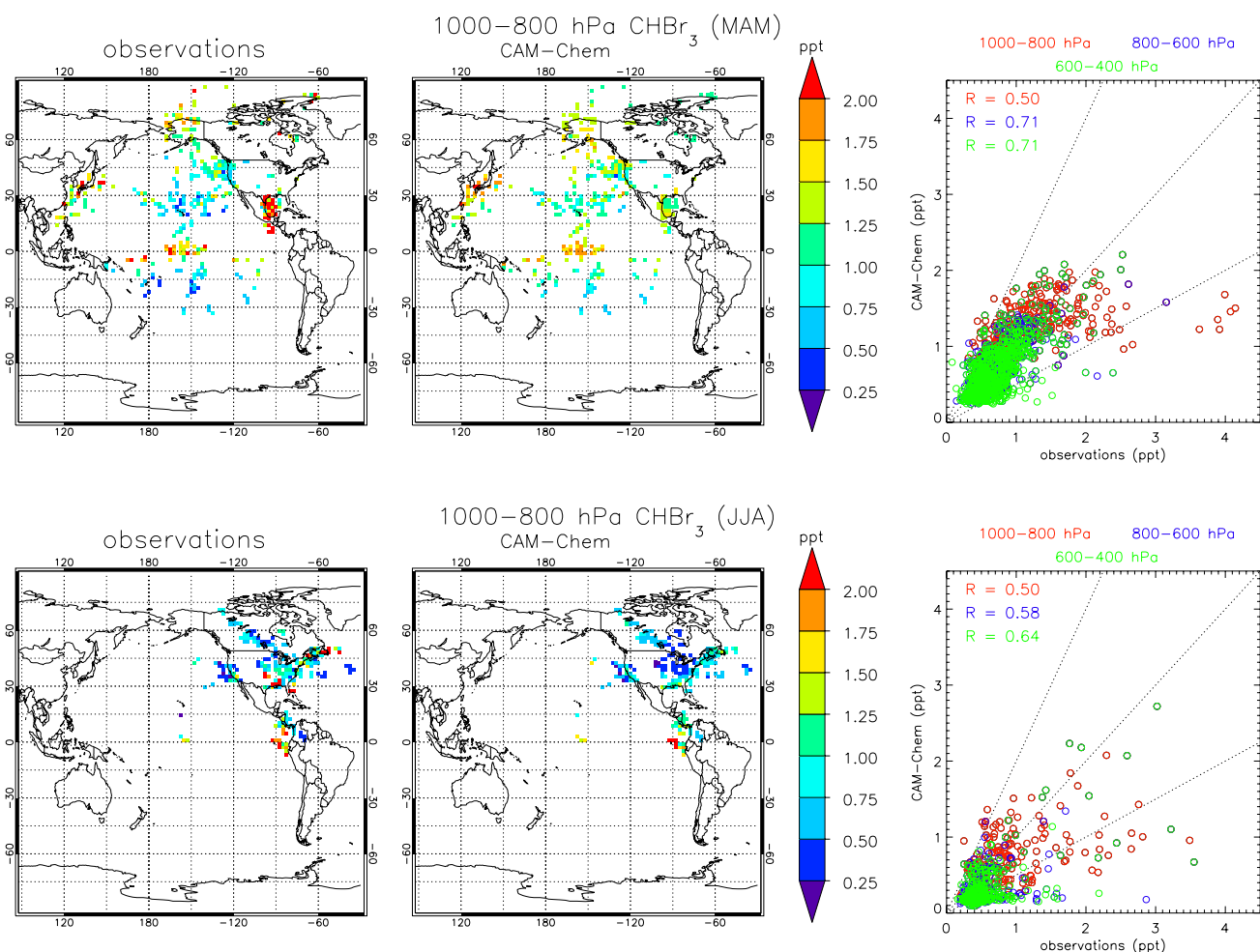


**Fig. 3.** Composite of (left) aircraft observations of  $\text{CHBr}_3$  and (centre) simulated  $\text{CHBr}_3$  in the lower-troposphere (1000–800 hPa) during (top) March–May and (bottom) June–August. The corresponding scatter-plots of simulated vs. observed  $\text{CHBr}_3$  during the same periods are shown on the right-hand side for 1000–800 hPa (red) as well as for two additional tropospheric layers (800–600 hPa, blue; 600–400 hPa, green);  $R$  represents the Pearson correlation coefficient for those layers. The 1:2, 1:1 and 2:1 lines are illustrated by dots. Model output was sampled at the same location and month as the observations, which in turn are averaged over the  $1.9^\circ$  (lat)  $\times$   $2.5^\circ$  (lon) horizontal grid cells of CAM-Chem.

In the case of  $\text{CH}_2\text{Br}_2$ , the estimated flux results from the compromise between reproducing the sparse aircraft observations in the SH and the 1994–2004 NOAA/CMDL cruise measurements over  $40^\circ$ – $60^\circ$  S (see Fig. 5). Hence, considering the good agreement with aircraft observations in the NH, the limited aircraft data available over southern latitudes where our estimate of the  $\text{CH}_2\text{Br}_2$  flux is small (10.6% of the total for  $20^\circ$ – $50^\circ$  S compared to 22.1% for  $20^\circ$ – $50^\circ$  N, see Table 4), and that our global total flux estimated for  $\text{CH}_2\text{Br}_2$  ( $67.3 \text{ Gg yr}^{-1}$ ) is similar to the  $62 \text{ Gg yr}^{-1}$  recently reported by Liang et al. (2010), we conclude that further observations in the southern latitudes are necessary to improve these estimates. Data from on-going and future aircraft campaigns such as the HIAPER Pole-to-Pole Observations (HIPPO) programme (Wofsy et al., 2011), which is

measuring atmospheric mixing ratios of trace gases with a pole-to-pole coverage within the troposphere and during all seasons, will be very valuable to improve the current emission estimates of VSL bromocarbons, in particular over the SH. Since data from the same aircraft campaigns have been exploited both to estimate and to evaluate VSL bromocarbon emission fluxes in this study, new observational datasets could also be used for an independent validation of the emission parameterisation presented here.

Overall, there is good agreement between modelled and observed mixing ratios of  $\text{CHBr}_2\text{Cl}$  and  $\text{CHBrCl}_2$ . Modelled  $\text{CH}_2\text{BrCl}$  remains low although within the range of variability of the observations for 600–400 hPa. Nevertheless, we calculate a global total flux of  $10 \text{ Gg yr}^{-1}$ , which is higher than the  $6.8 \text{ Gg yr}^{-1}$  reported by Warwick et al. (2006a) and

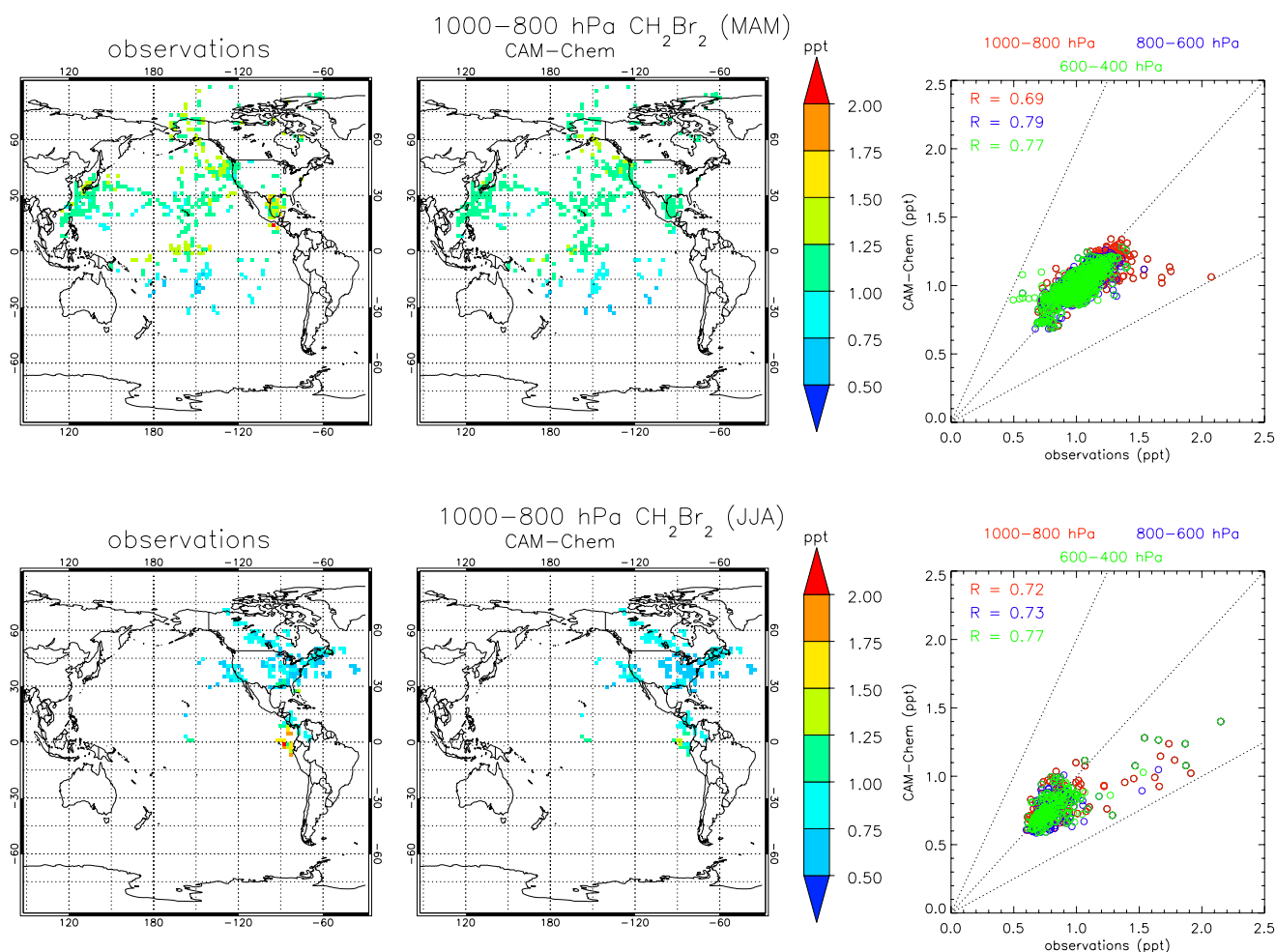
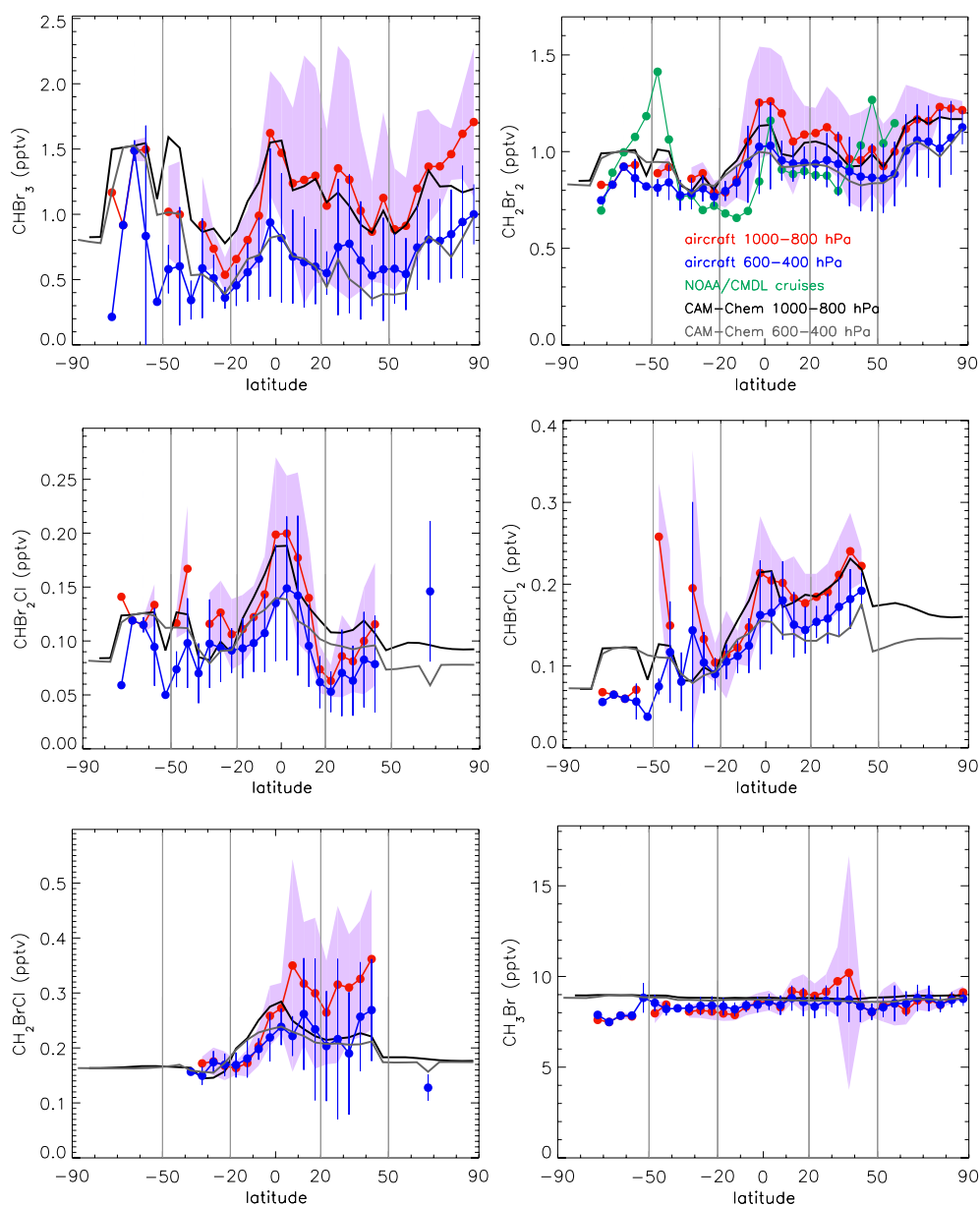


Fig. 4. Same as Fig. 3 but for  $\text{CH}_2\text{Br}_2$ .

Kerkweg et al. (2008) (Table 3). The latitudinal distribution shown in Fig. 5 and the comparisons with vertical profiles from the very few campaigns with  $\text{CH}_2\text{BrCl}$  data available (not shown) suggest a closer match between model and observations for the mid-troposphere (e.g. 600–400 hPa) than for the lower troposphere (e.g. 1000–800 hPa). This indicates that the model cannot reproduce the shape of the vertical profile for  $\text{CH}_2\text{BrCl}$ . Finally, with the lower boundary condition of 9 ppt imposed to  $\text{CH}_3\text{Br}$  the model results are within the uncertainty of the observations in the NH but slightly overestimate the more sparse observations in the SH. A more detailed analysis of  $\text{CH}_3\text{Br}$  vertical profiles is included in Sect. 5.2.

We have shown that the use of the same chl-*a* dependent parameterisation for all VSL halocarbons, with elevated emission fluxes within 20° N–20° S, enables the model to capture the maximum atmospheric mixing ratios of bromocarbons observed in the tropics. However the observed maximum is shifted towards the northern tropics while it is centred on the Equator in the model. This parameterisation is

an attempt to represent the known biogenic sources of halocarbons from micro and macroalgae, but the different VSL halocarbon species might not have exactly the same sources (e.g. different types of macroalgae and phytoplankton as well as different chemical processes). In addition, other environmental factors such as the content of DOM in water, the solar radiation flux at the surface or the wind speed are not considered here. The zonal emission approach adopted outside the tropics is an even more simplified representation that obviously leads to the under- and overestimation of the atmospheric mixing ratios of VSL halocarbons over different regions within the same latitudinal bands, which tend to compensate each other. The 2.5 emission ratio between coastal and oceanic areas in the extratropics has been adopted to account for the high coastal emission sources in a simple way, but this will not necessarily reproduce the real regional patterns of halocarbon emissions. A comprehensive parameterisation of processes at the sea-ice interface would also be required for the representation of emissions in the polar areas.



**Fig. 5.** Latitudinal dependence of the observed and modelled bromocarbons  $\text{CHBr}_3$ ,  $\text{CH}_2\text{Br}_2$ ,  $\text{CHBr}_2\text{Cl}$ ,  $\text{CHBrCl}_2$ ,  $\text{CH}_2\text{BrCl}$  and  $\text{CH}_3\text{Br}$  averaged for each  $2.5^\circ$  latitudinal band within 1000–800 hPa and 600–400 hPa. When at least two data points are available for a given latitudinal band, shaded areas and vertical bars indicate standard deviations of the aircraft observations for 1000–800 hPa and 600–400 hPa, respectively. Model output corresponds to the location and month of the aircraft observations when available, otherwise all CAM-Chem output for that latitude is used. In the case of  $\text{CH}_2\text{Br}_2$ , observations from NOAA/CMDL vessels from 1994 to 2004 are also shown in green colour.

## 5.2 Vertical profiles of selected species: $\text{CHBr}_3$ , $\text{CH}_2\text{Br}_2$ , $\text{CH}_3\text{Br}$ and $\text{CH}_3\text{I}$

Figures 7, 8, 9 and 10 illustrate the observed and modelled vertical profiles for the major VSL bromocarbons ( $\text{CHBr}_3$  and  $\text{CH}_2\text{Br}_2$ ), the most abundant brominated gas in the free troposphere ( $\text{CH}_3\text{Br}$ ) and  $\text{CH}_3\text{I}$ . Profiles are shown for independent aircraft missions and separately for the troposphere

(surface–200 hPa) and the upper troposphere – lower stratosphere (UTLS, 300–50 hPa) region, where convection could deliver some portion of these gases and their breakdown products.

There is a good agreement between observed and simulated  $\text{CHBr}_3$  throughout the troposphere for all campaigns (Fig. 7). The mean simulated field underestimates the observations from TRACE-P and INTEX-A, but lies within the

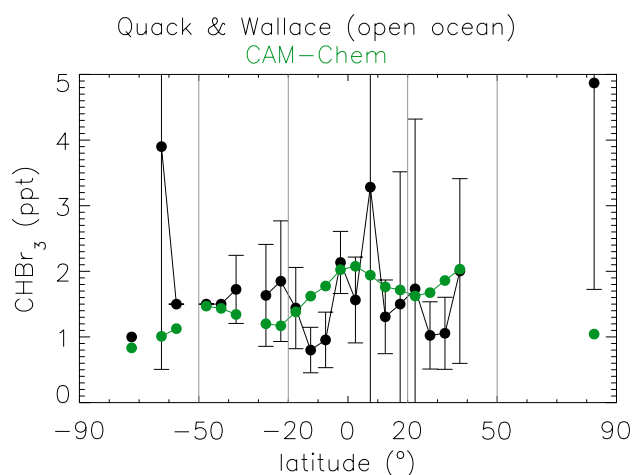


**Fig. 6.** Latitudinal dependence of observed and simulated bromoform atmospheric mixing ratios at the surface. Black circles and vertical bars represent mean and standard deviations of measurements over the open ocean in Table 2 of Quack and Wallace (2003). Green circles depict zonally averaged CAM-Chem output at the lowest model level for grid cells over ocean.

range of variability of the measurements. The variability in the model (given by horizontal bars) is somewhat small compared to that of the measurements (indicated by the shaded area) in the case of some aircraft campaigns. This is expected for a relatively short-lived compound such as  $\text{CHBr}_3$ , considering the constant oceanic emission fields implemented for those latitudinal bands outside the tropics, and the fact that the coarse grid cell of the model cannot capture the variability of the observations. Another reason could be the use of a single 1-yr model simulation with climatological SSTs. The model matches the average mixing ratios and the shape of the  $\text{CHBr}_3$  profiles observed in the UTLS region, with the exception of the overestimation of the measurements from the oldest aircraft campaign used here (STRAT, 1996).

Similarly to  $\text{CHBr}_3$ , modelled  $\text{CH}_2\text{Br}_2$  is very close to the observations throughout most of the troposphere. However the model starts to deviate from the observations in the mid- to upper-troposphere, and consistently overestimates them in the UTLS region (Fig. 8). In particular, the model over-predicts  $\text{CH}_2\text{Br}_2$  by  $\sim 70\%$  within 150–50 hPa. A similar behaviour is found for  $\text{CH}_2\text{BrCl}$  (not shown), which is the most long-lived of the VSL halocarbons (atmospheric lifetime of  $\sim 145$  days, compared to  $\sim 130$  days for  $\text{CH}_2\text{Br}_2$ ); however the number of measured vertical profiles for  $\text{CH}_2\text{BrCl}$  is much smaller. A high bias for  $\text{CH}_2\text{Br}_2$  within 150–50 hPa has also been found in the GEOS Climate Chemistry Model (GEOS CCM) by Liang et al. (2010), who attributed it to a possibly low OH field in the model. In addition, a simulation of the atmospheric chemistry general circulation model ECHAM5/MESy overestimated the amount of  $\text{CH}_2\text{Br}_2$  measured at cruise altitude (9–11 km)

within CARIBIC1 by a factor of approximately 1.5 (Kerkweg et al., 2008). The coincidence in the overestimation of  $\text{CH}_2\text{Br}_2$  in the proximity of the UTLS for the three models needs further investigation. Hossaini et al. (2010) showed that the loss of  $\text{CH}_2\text{Br}_2$  throughout the troposphere is dominated by reaction with OH, with photolysis being slow, while the two loss channels are roughly equal at  $\sim 100$  hPa, and photolysis is the dominant loss process above. In CAM-Chem,  $\text{CH}_2\text{Br}_2$  is larger than the observations at  $\sim 150$  hPa for most campaigns, which indicates that other mechanisms than photolysis should be responsible for the overestimation in the model. Sensitivity simulations conducted by Hossaini et al. (2010) suggest that  $\text{CH}_2\text{Br}_2$  injection in the TTL is not very sensitive to model parameterised convection, while they found the impact of the modelled OH field to be significant. We have compared the prescribed OH field used in the simulation presented here with that from a full chemistry CAM-Chem simulation. On average for the periods and areas shown in Fig. 8, the prescribed OH field is around 85 % of the modelled value within 300–100 hPa, which could only partly explain the overestimation of  $\text{CH}_2\text{Br}_2$ . Another plausible source of error in the model might be the rate constant estimated for the reaction  $\text{CH}_2\text{Br}_2 + \text{OH}$ . The activation energy recommended by Sander et al. (2006) for this reaction has been determined with an uncertainty of  $\pm 12\%$  for 243–380 K (Mellouki et al., 1992; Atkinson et al., 2008), while atmospheric temperatures for altitudes above 250 hPa are well below 240 K. Rate constants are usually known with minimum uncertainty at room temperature while the overall uncertainty normally increases at lower temperatures. The application of the uncertainty estimates derived by Sander et al. (2006) reveals a considerable uncertainty in the rate constant for  $\text{CH}_2\text{Br}_2$  (e.g.  $\sim 30\%$  at around 240 K), somewhat higher than that for  $\text{CH}_3\text{Br}$  and  $\text{CH}_2\text{BrCl}$  ( $\sim 20\%$ ). Hossaini et al. (2010) also highlighted the strong impact of the vertical transport calculation in the lower stratosphere region on the residence times and predicted mixing ratios of  $\text{CH}_2\text{Br}_2$  in the TTL. They concluded that vertical transport calculated from diagnosed heating rates above 350 K in a  $\theta$ -coordinate model (SLIMCAT) is more realistic than that calculated from ECMWF analysed divergence fields in a p-coordinate model (TOMCAT) since the latter one exhibits too rapid vertical motion. CAM-Chem does not use analysed meteorological fields, but it is quite likely that the residence times of air masses in the UTLS will have an impact on the  $\text{CH}_2\text{Br}_2$  field predicted by the model for that region of the atmosphere; however this could also affect other species for which we found a better agreement with observations in that region.

The  $\text{CH}_3\text{Br}$  field simulated by CAM-Chem is close to the observations from all aircraft missions in the troposphere (Fig. 9), with the exception of some overestimation for INTEX-A and INTEX-B. However the variability in the model is small compared to that of the observations. The lower boundary condition imposed for this species in the model may not fully capture the regional and temporal

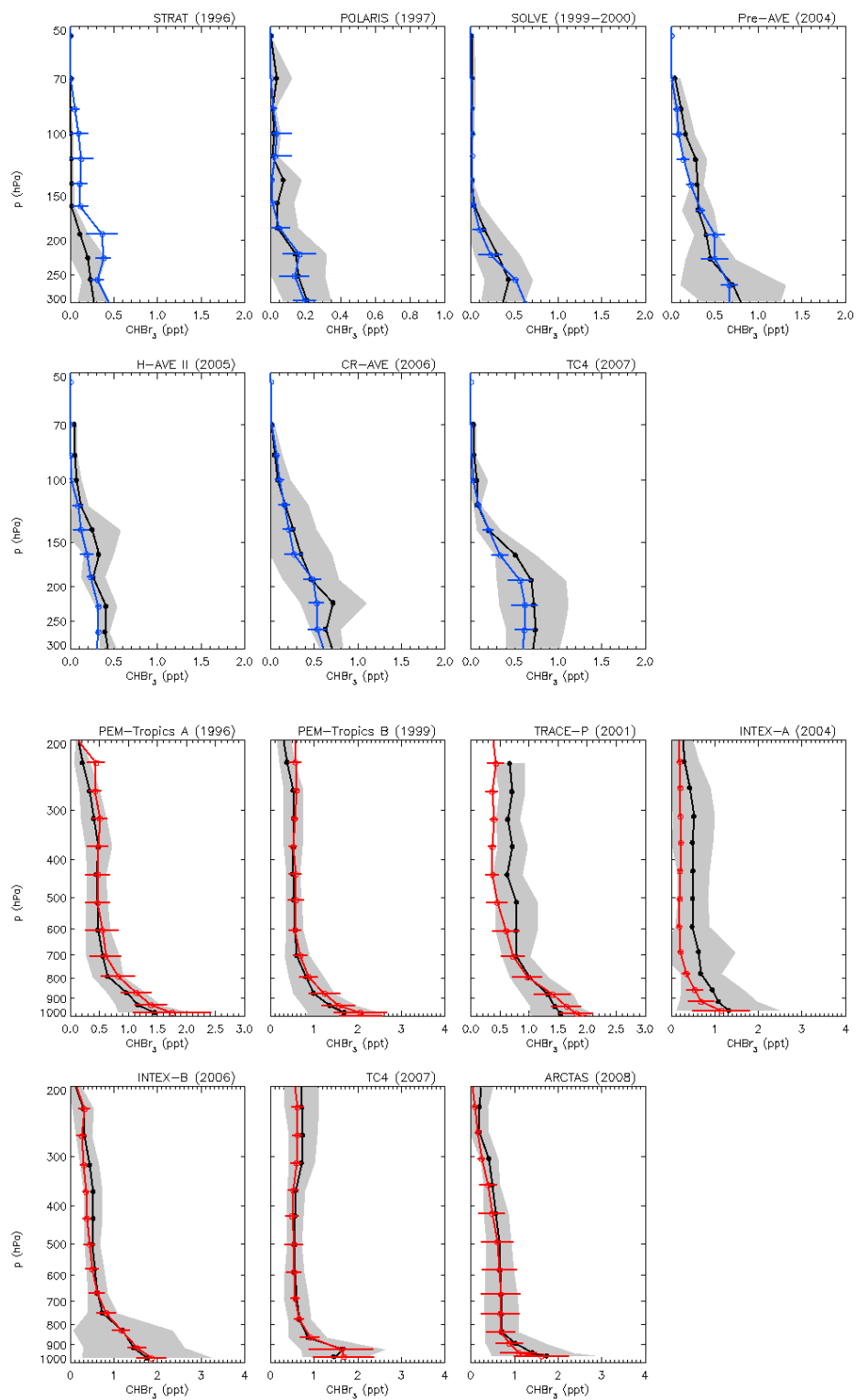


**Fig. 7.** Comparison of observed and simulated vertical profiles of  $\text{CHBr}_3$  for a number aircraft missions in the UTLS region and the troposphere. Black lines and grey shaded areas indicate the mean and one standard deviation of the observations. Blue (red) lines and horizontal bars show the mean and one standard deviation of the simulated  $\text{CHBr}_3$  field at the same locations and during the same months as the observations in the UTLS (troposphere).

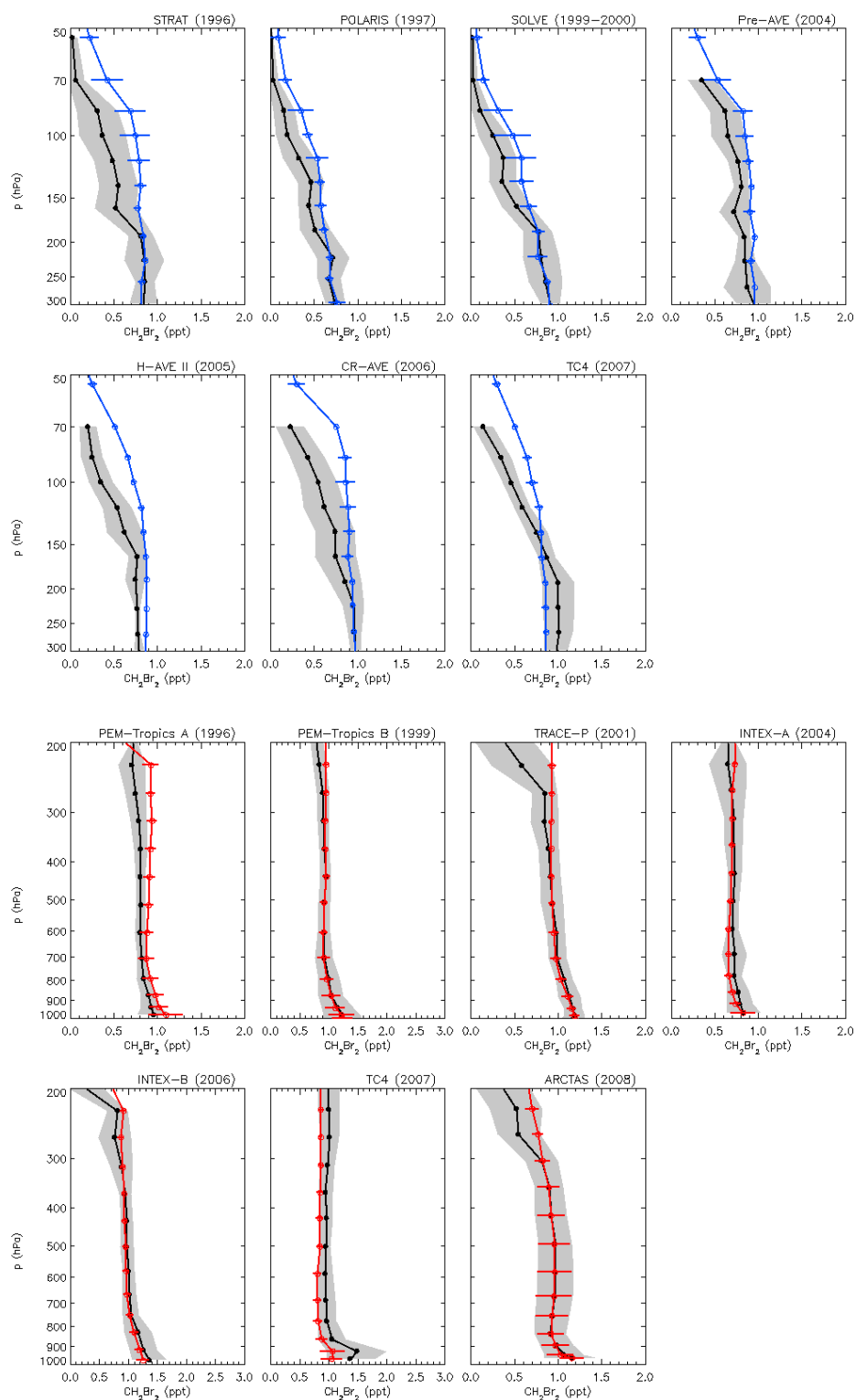


Fig. 8. As Fig. 7 but for  $\text{CH}_2\text{Br}_2$ .

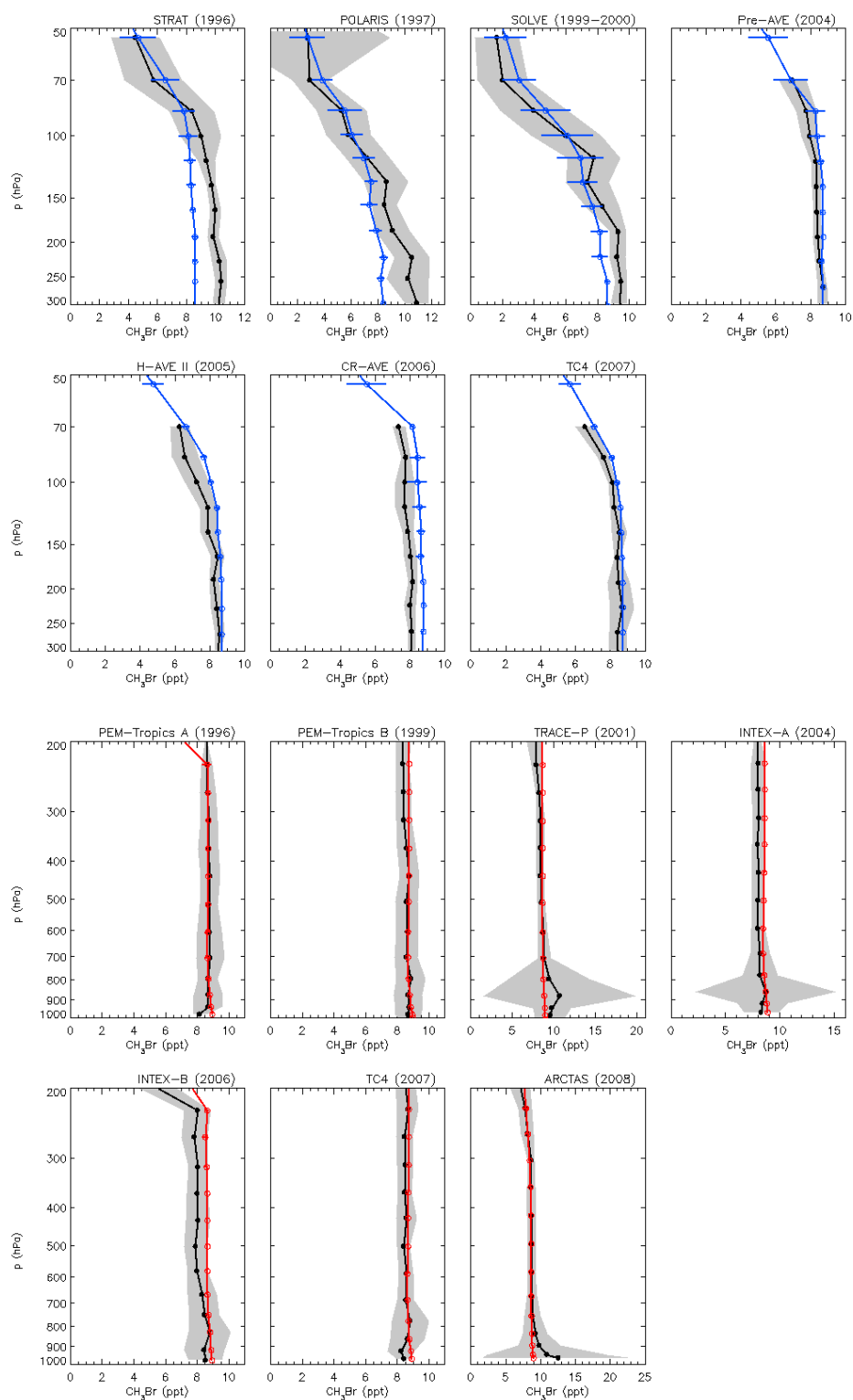
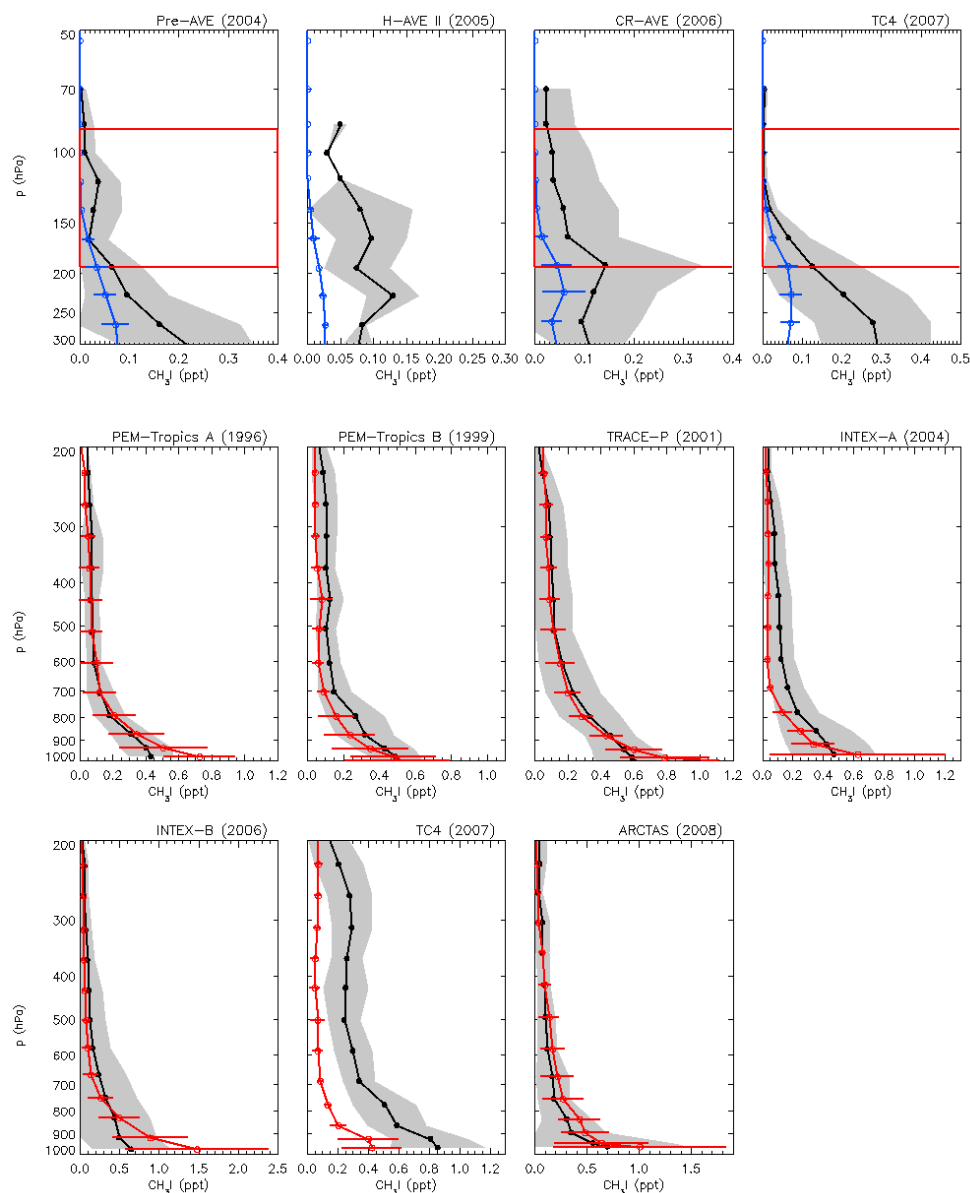


Fig. 9. As Fig. 7 but for  $\text{CH}_3\text{Br}$ .



**Fig. 10.** As Fig. 7 but for  $\text{CH}_3\text{I}$ . In the case of the UTLS plots, the position of the tropical tropopause layer (TTL), between around 12 and 17 km altitude, is illustrated by red lines for those aircraft missions with sufficient data over the tropics.

variability found in the observations. Some of the deviations between model and observations might also be related to the use of climatological SSTs and to the fact that the model simulation does not intend to reproduce the meteorological years when the campaigns were conducted. The model generally matches the shape of the vertical profile and the overall mixing ratios observed in the UTLS region, with deviations within 20 % of the observations. Unlike  $\text{CH}_2\text{Br}_2$ , no consistent bias of either positive or negative sign is found for any vertical level in this region, providing some confidence in the transport and the OH field prescribed in the model. Noticeably, CAM-Chem underestimates the observations between

300 and 100 hPa only for the campaigns that were conducted in the late 1990s (STRAT, in 1996; POLARIS, in 1997, and SOLVE, in late 1999–early 2000), where an average mixing ratio of  $\sim 10$  pptv was observed at 300 hPa, while the model overestimates observations since 2004. These results may be due to the fact that  $\text{CH}_3\text{Br}$  is specified in the model to reproduce the observed surface concentrations for 2000 (9 pptv), while there is evidence that  $\text{CH}_3\text{Br}$  has declined as a result of reduced industrial production since the peak levels measured during 1996–1998 (WMO, 2011). Some deviations might also be related to the geographical region and time of year covered by each campaign. As an example, emissions

and atmospheric mixing ratios of  $\text{CH}_3\text{Br}$  are higher in the northern than in the Southern Hemisphere, particularly before they started to decline (WMO, 2011), while we have imposed the same lower boundary condition everywhere on the globe. Ideally, this boundary condition should be time-dependent to account for the observed decline in atmospheric mixing ratios and also possibly meridionally-varying in order to reproduce the observed inter-hemispheric differences.

Modelled  $\text{CH}_3\text{I}$  mixing ratios lie within the range of variability of the observations in the troposphere for most campaigns (Fig. 10), although on the low side for some of them (e.g. PEM Tropics-B and INTEX-A) and considerably lower during TC4. This aircraft campaign covered a region around Central America, including the most northern part of South America, the south of North America and the surrounding Atlantic and Pacific coasts. The average  $\text{CH}_3\text{I}$  mixing ratios observed during TC4 are around 0.6–0.8 pptv in the lower troposphere and close to 0.3 pptv at around 300 hPa, larger than in the other flights that took place in the tropics. It is possible that there are strong local sources of either oceanic or terrestrial origin influencing measurements during this campaign that cannot be accounted for by the emission inventory of Bell et al. (2002). However the zonal approach used here to estimate bromocarbon emissions also presents difficulties to reproduce the levels of some species such as  $\text{CH}_2\text{Br}_2$  (see Fig. 8),  $\text{CHBrCl}_2$  and  $\text{CHBr}_2\text{Cl}$  (not shown) in the troposphere during TC4. Note that TC4 occurred during an incipient La Niña event, with cooler sea surface temperatures than normal as well as with convective activity less intense and with a distribution different from the mean climatology (Pfister et al., 2010). Therefore it is possible that the untypical meteorological conditions during that campaign are partly responsible for the discrepancies between modelled and observed  $\text{CH}_3\text{I}$ . Despite the underestimation of  $\text{CH}_3\text{I}$  throughout most of the troposphere for the above-mentioned campaigns, CAM-Chem tends to overestimate aircraft observations in the lower troposphere.

Finally, it is worth noting that the modelled  $\text{CH}_3\text{I}$  mixing ratios are considerably lower than the observations for all campaigns in the UTLS. Due to its relatively short lifetime, methyl iodide is unlikely to reach the TTL, unless emitted directly into deep convection cells. Interestingly, observations indicate the unambiguous presence of  $\text{CH}_3\text{I}$  in the TTL, with average mixing ratios of around 0.1 ppt in the lowermost part of this layer, while the modelled  $\text{CH}_3\text{I}$  field is consistently lower than the observations. The modelling of  $\text{CH}_3\text{I}$  in the UTLS requires a good characterisation of the emissions over tropical areas where it can be transported to the TTL by deep convection. Field data from seven cruises across the Atlantic, Pacific, and Southern Oceans suggest a global oceanic source of  $\sim 610 \text{ Gg yr}^{-1}$  (Butler et al., 2007), around double than the global  $\text{CH}_3\text{I}$  flux used here. This illustrates the significant uncertainty in the emission sources. Over the last years changes have been made to the deep convection scheme of the model (Zhang and McFarlane, 1995) by including

the effects of deep convection in the momentum equation (Richter and Rasch, 2008) and using a dilute approximation in the plume calculation (Neale et al., 2008). They result in a much improved representation of deep convection that occurs considerably less frequently, but is much more intense compared to older versions of the model (Gent et al., 2011). No strong biases in the tropical upper-troposphere that would indicate a lack of deep convection have been reported for CAM-Chem (e.g. Lamarque et al., 2011). It is also worth noting that the model includes UV absorption cross sections of  $\text{CH}_3\text{I}$  at 298 K. If the temperature dependence of such absorption cross sections was considered this would reduce the photodissociation rate constants and therefore increase the lifetime of this species (Roehl et al., 1997). Ongoing work will address the impact of the emission strength and distribution as well as of the parameterisations of convection and photochemistry on the modelling of  $\text{CH}_3\text{I}$ .  $\text{CH}_2\text{Br}_2$  and  $\text{CH}_3\text{I}$  are, respectively, the most abundant VSL bromocarbon and iodocarbon in the stratosphere. The discrepancies between modelled and observed fields of these two species in the UTLS need further investigation, together with a detailed analysis of inorganic bromine and iodine species, before the impact of VSL halogen sources on stratospheric ozone can be properly quantified with CAM-Chem. Such analyses are out of the scope of this paper.

### 5.3 Iodine-containing dihalomethanes ( $\text{CH}_2\text{IX}$ )

The three shortest lived iodocarbons explicitly implemented in CAM-Chem ( $\text{CH}_2\text{ICl}$ ,  $\text{CH}_2\text{IBr}$ ,  $\text{CH}_2\text{I}_2$ ) have very short lifetimes of hours to minutes and are therefore relevant as sources of reactive halogens in the MBL. As described in Sect. 4, their total emission fluxes have been determined following previous reports and comparisons with available observations in the MBL (see Table 2). Such measurements are very sparse, in particular for  $\text{CH}_2\text{IBr}$  and  $\text{CH}_2\text{I}_2$ . The results of these comparisons are shown in Fig. 11. Overall, the agreement is good for  $\text{CH}_2\text{ICl}$  (atmospheric lifetime of  $\sim 8 \text{ h}$ ) since the modelled field is within the variability of the observations for most locations. Similar results are found for  $\text{CH}_2\text{IBr}$  (lifetime of  $\sim 2.5 \text{ h}$ ), except for the strong underestimation at the coastal and shelf locations in northern mid- and high-latitudes. Possible explanations for the underestimation of the mixing ratios over areas with strong sources are some of the simplifications used in our approach, such as the extrapolation of the results of Jones et al. (2010), which are reported with a high degree of uncertainty, and more likely the assumption of a constant 2.5 larger flux over coast compared to open ocean. A sensitivity simulation with a coast-to-ocean emission ratio of 5 for all  $\text{CH}_2\text{IX}$  species brings the modelled  $\text{CH}_2\text{IBr}$  mixing ratios closer to observations, but it also results in an overall overestimation of  $\text{CH}_2\text{ICl}$ . This shows the difficulties involved in simulating the spatial features of such short-lived compounds by using global models of coarse horizontal and vertical resolution.

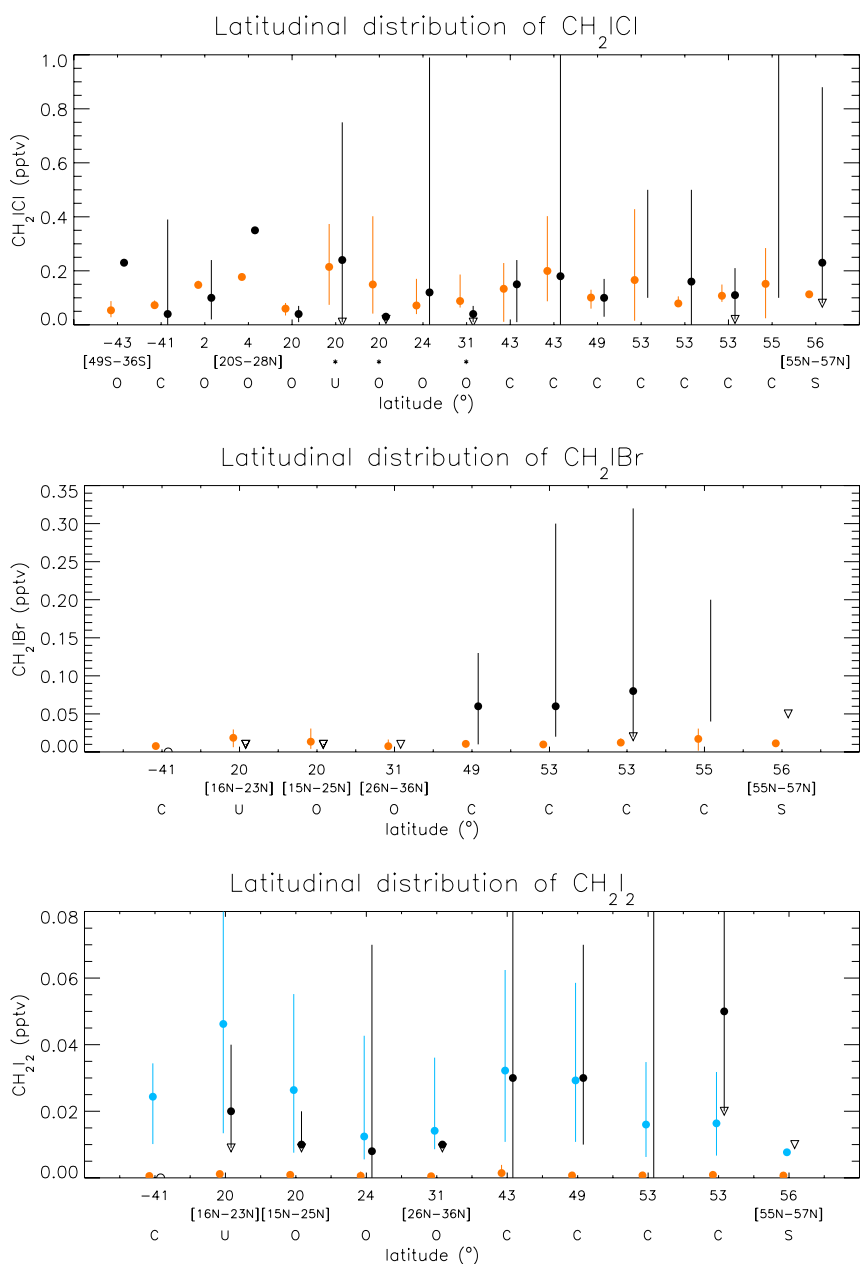


**Fig. 11.** Comparison of observed (black) and modelled (orange) mixing ratios of  $\text{CH}_2\text{ICl}$  (top),  $\text{CH}_2\text{IBr}$  (middle) and  $\text{CH}_2\text{I}_2$  (bottom). The observations, which are also summarised in Table 2, have been ordered along the x-axis according to their latitude from South to North. The range of latitudes is shown in brackets if the observations cover a region instead of a single point (this is sometimes indicated by stars in the case of  $\text{CH}_2\text{ICl}$  due to reasons of space). They have been classified as open ocean (O), upwelling (U), shelf (S), and coast (C). The full black circles represent the average of the observed values and the black bars correspond to their range, given by the minimum–maximum or by the 10th–90th percentiles depending on the dataset. The minimum observed value is indicated by an open triangle when it corresponds to an upper limit, while some very low observations on a cliff-top location (expected to be lower estimates) are depicted by an open circle. Orange circles represent the average modelled fields for the location and month(s) of the observations. When observations cover a geographical region the minimum and maximum monthly modelled values over that area are also depicted by orange bars; otherwise the mean, minimum and maximum of the monthly modelled fields on the 9 model grid cells closest to the location of the measurements are plotted. In the case of  $\text{CH}_2\text{I}_2$ , results from an additional model simulation are shown in blue to reflect the importance of the daily cycle of emissions for these species (see details in text).

For the emission of  $\text{CH}_2\text{IX}$  species we follow a solar diurnal profile, with emissions peak in the early afternoon and null emissions at night. Following this emission profile, the model largely underestimates the observations of  $\text{CH}_2\text{I}_2$  (lifetime of  $\sim 7$  min) since most of the  $\text{CH}_2\text{I}_2$  emitted in the model at daytime is lost by photolysis in only a few minutes, resulting in very low modelled  $\text{CH}_2\text{I}_2$  mixing ratios (Fig. 11, bottom). As a sensitivity test we injected the same  $\text{CH}_2\text{I}_2$  flux using a weaker emission cycle, with a nighttime emission flux half of that during daytime. As a consequence of the injection of moderately small amounts of  $\text{CH}_2\text{I}_2$  at night, the monthly average concentrations considerably increase, leading to an overall better agreement with observations (Fig. 11, bottom). This illustrates that a good knowledge of the shape of the diurnal emission profile is necessary to estimate the source strength of the shortest lived iodocarbons.

Further field campaigns focusing on the simultaneous observation of these iodocarbons in air and water are needed to gain a better understanding of the strength and spatio-temporal distribution of their sources, and therefore improve their representation in atmospheric models.

## 6 Summary and conclusions

We have implemented natural oceanic sources of VSL halocarbons and a detailed chemical scheme of bromine and iodine in a global chemistry-climate model. The same parameterisation of emissions has been used for all VSL bromocarbons and iodocarbons treated in the model, with the exception of  $\text{CH}_3\text{I}$  and  $\text{CH}_3\text{Br}$ . This consists of a biogenic chl-*a* dependent source in the tropical oceans ( $20^\circ\text{N}$ – $20^\circ\text{S}$ ), constant oceanic fluxes for four latitudinal bands in the extratropics ( $90^\circ$ – $50^\circ\text{S}$ ,  $50^\circ$ – $20^\circ\text{S}$ ,  $20^\circ$ – $50^\circ\text{N}$ , and  $50^\circ$ – $90^\circ\text{N}$ ) with coastal emission fluxes 2.5 times higher than over the ocean, and no emissions at the sea-ice interface in the high latitudes. Halocarbon measurements from a number of aircraft campaigns and some available observations in the MBL have been used to derive the emission fluxes of bromocarbons and iodocarbons. The limitations of this approach have been discussed. The model also includes emissions of  $\text{CH}_3\text{I}$  from the inventory of Bell et al. (2002), which accounts for both oceanic sources of photochemical origin and terrestrial sources, while the longer lived  $\text{CH}_3\text{Br}$  is relaxed to a constant lower boundary condition to simplify the source optimisation of halocarbons.

The global total emission fluxes of  $\text{CHBr}_3$  ( $533\text{ Gg yr}^{-1}$ ) and  $\text{CH}_2\text{Br}_2$  ( $67.3\text{ Gg yr}^{-1}$ ) estimated with CAM-Chem are within the range of values given by previous modelling studies (Yang et al., 2005; Warwick et al., 2006a; Kerkweg et al., 2008; Liang et al., 2010). The emission estimates for the other three VSL bromocarbons included in the model ( $\text{CH}_2\text{BrCl}$ ,  $\text{CHBr}_2\text{Cl}$  and  $\text{CHBrCl}_2$ ) are within 30% agreement with previously reported estimates. The global total fluxes of iodocarbons in this study are equivalent to those of

Bell et al. (2002) for  $\text{CH}_3\text{I}$  and Jones et al. (2010) for  $\text{CH}_2\text{ICl}$ ,  $\text{CH}_2\text{IBr}$  and  $\text{CH}_2\text{I}_2$ .

In general, the latitudinal distributions of the observed and simulated atmospheric mixing ratios of VSL bromocarbons agree within the range of variability of the measurements. The use of a chl-*a* dependent parameterisation for all VSL halocarbons, with elevated emission fluxes within  $20^\circ\text{N}$ – $20^\circ\text{S}$ , enables the model to capture the maximum atmospheric mixing ratios of bromocarbons observed in the tropics. However, we have identified that the geographical coverage of the available aircraft observations is insufficient to correctly characterise the emission fluxes in the southern extratropics. Surface observations from Quack and Wallace (2003) for  $\text{CHBr}_3$  and NOAA/CMDL vessel data for  $\text{CH}_2\text{Br}_2$  have proven to be useful to fill in some observational data gaps, but the use of these data has also reflected the difficulties in reconciling observations of VSL halocarbons from different sources.

Overall the vertical profiles of bromocarbons and  $\text{CH}_3\text{I}$  simulated by CAM-Chem are in good agreement with observations in the troposphere and the UTLS region, in particular for the most relevant VSL bromocarbon in the troposphere, i.e.  $\text{CHBr}_3$ . However there are some remaining issues such as the overestimation of  $\text{CH}_2\text{Br}_2$  in the UTLS, and the underestimation of  $\text{CH}_3\text{I}$  for the same region and to a lesser extent for some campaigns in the troposphere. We have discussed a number of factors – mainly the rate constants estimated for the reaction of  $\text{CH}_2\text{Br}_2$  with OH, but also the prescribed OH field used and the residence times of air masses in the UTLS inside the model – that might impact on the  $\text{CH}_2\text{Br}_2$  field simulated in the UTLS. A detailed evaluation of the emission inventory used for  $\text{CH}_3\text{I}$ , of convection and photochemistry in the model, and of the meteorological conditions for the individual field campaigns may be needed to understand the deviations between observed and simulated  $\text{CH}_3\text{I}$ . The constant lower boundary condition used for the longer-lived  $\text{CH}_3\text{Br}$  is sufficient to reasonably reproduce the observed mixing ratios, but it would be necessary to run the model for a multiannual period with time-varying lower boundary conditions to account for the known decline in the anthropogenic sources of this species. Despite the difficulties involved in the global modelling of the shortest lived iodocarbons ( $\text{CH}_2\text{ICl}$ ,  $\text{CH}_2\text{IBr}$ ,  $\text{CH}_2\text{I}_2$ ), whose sea-to-air fluxes and atmospheric abundances are not well constrained, results from comparisons of the modelled fields with published observations in the MBL are reasonable. Some sensitivity simulations have proven that the diurnal cycle of emissions for these species, in particular for  $\text{CH}_2\text{I}_2$ , is key when assessing the total amounts released to the atmosphere.

This study presents the first implementation of bromine and iodine oceanic sources from VSL halocarbons in a global chemistry-climate model. The companion paper by Saiz-Lopez et al. (2011) uses CAM-Chem and radiative transfer calculations to estimate the radiative impact resulting

from halogen-driven tropospheric ozone loss over the tropical oceans. Future work will investigate the importance of the bromine release from sea salt aerosol as well as the potential of VSL bromine and iodine species to influence the oxidation power of the atmosphere by modifying the atmospheric burden of trace gases and aerosols.

**Supplementary material related to this article is available online at:**

<http://www.atmos-chem-phys.net/12/1423/2012/acp-12-1423-2012-supplement.pdf>

*Acknowledgements.* This work was funded by the Spanish Research Council (CSIC) and the Regional Government of Castilla-La Mancha. D. K. was partially funded by the Department of Energy under the SciDAC program. The CESM project is supported by the National Science Foundation and the Office of Science (BER) of the US Department of Energy. The National Center for Atmospheric Research is operated by the University Corporation for Atmospheric Research under sponsorship of the National Science Foundation. We are grateful to Nadine Unger for providing the CH<sub>3</sub>I emission data set.

Edited by: S. Kloster

## References

- Atkinson, R., Baulch, D. L., Cox, R. A., Hampson, R. F., Kerr, J. A., Rossi, M. J., and Troe, J.: Evaluated Kinetic and Photochemical Data for Atmospheric Chemistry: Supplement VIII, Halogen Species Evaluation for Atmospheric Chemistry, *J. Phys. Chem. Ref. Data*, 29, 167, doi:10.1063/1.556058, 2000.
- Atkinson, R., Baulch, D. L., Cox, R. A., Crowley, J. N., Hampson Jr., R. F., Hynes, R. G., Jenkin, M. E., Kerr, J. A., Rossi, M. J., and Troe, J.: Summary of evaluated kinetic and photochemical data for atmospheric chemistry: web version February 2006, available at: <http://www.iupac-kinetic.ch.cam.ac.uk>, 2006.
- Atkinson, R., Baulch, D. L., Cox, R. A., Crowley, J. N., Hampson, R. F., Hynes, R. G., Jenkin, M. E., Rossi, M. J., Troe, J., and Wallington, T. J.: Evaluated kinetic and photochemical data for atmospheric chemistry: Volume IV – gas phase reactions of organic halogen species, *Atmos. Chem. Phys.*, 8, 4141–4496, doi:10.5194/acp-8-4141-2008, 2008.
- Atlas, E., Pollock, W., Greenberg, J., Heidt, L., and Thompson, A. M.: Alkyl nitrates, nonmethane hydrocarbons, and halocarbon gases over the equatorial Pacific Ocean during Saga-3, *J. Geophys. Res.*, 98, 16933–16947, 1993.
- Baker, J. M., Sturges, W. T., Sugier, J., Sunnenberg, G., Lovett, A. A., Reeves, C. E., Nightingale, P. D., and Penkett, S. A.: Emissions of CH<sub>3</sub>Br, organochlorines, and organoiodines from temperate macroalgae, *Chemosphere Global Change Sci.*, 3, 93–106, 2001.
- Bell, N., Hsu, L., Jacob, D. J., Schultz, M. G., Blake, D. R., Butler, J. H., King, D. B., Lobert, J. M., and Maier-Reimer, E.: Methyl iodide: Atmospheric budget and use as a tracer of marine convection in global models, *J. Geophys. Res.*, 107, 4340, doi:10.1029/2001JD001151, 2002.
- Bilde, M., Wallington, T. J., Ferronato, C., Orlando, J. J., Tyndall, G. S., Estupiñan, E., and Haberkorn, S.: Atmospheric Chemistry of CH<sub>2</sub>BrCl, CHBrCl<sub>2</sub>, CHBr<sub>2</sub>Cl, CF<sub>3</sub>CHBrCl, and CBr<sub>2</sub>Cl<sub>2</sub>, *J. Phys. Chem. A*, 102, 1976–1986, 1998.
- Bloss, W. J., Lee, J. D., Johnson, G. P., Sommariva, R., Heard, D. E., Saiz-Lopez, A., Plane, J. M. C., McFiggans, G., Coe, H., Flynn, M., Williams, P., Rickard, A. R., and Fleming, Z. L.: Impact of halogen monoxide chemistry upon boundary layer OH and HO<sub>2</sub> concentrations at a coastal site, *Geophys. Res. Lett.*, 32, L06814, doi:10.1029/2004GL022084, 2005.
- Boucher, O., Moulin, C., Belviso, S., Aumont, O., Bopp, L., Cosme, E., von Kuhlmann, R., Lawrence, M. G., Pham, M., Reddy, M. S., Sciare, J., and Venkataraman, C.: DMS atmospheric concentrations and sulphate aerosol indirect radiative forcing: a sensitivity study to the DMS source representation and oxidation, *Atmos. Chem. Phys.*, 3, 49–65, doi:10.5194/acp-3-49-2003, 2003.
- Brioude, J., Portmann, R. W., Daniel, J. S., Cooper, O. R., Frost, G. J., Rosenlof, K. H., Granier, C., Ravishankara, A. R., Montzka, S. A., and Stohl, A.: Variations in ozone depletion potentials of very short-lived substances with season and emission region, *Geophys. Res. Lett.*, 37, L19804, doi:10.1029/2010GL044856, 2010.
- Butler, J. H., King, D. B., Lobert, J. M., Montzka, S. A., Yvon-Lewis, S. A., Hall, B. D., Nicola, J., Warwick, N. J., Mondeel, D. J., Aydin, M., and Elkins, J. W.: Oceanic distributions and emissions of short-lived halocarbons, *Global Biogeochem. Cy.*, 21, GB1023, doi:10.1029/2006GB002732, 2007.
- Calvert, J. G. and Lindberg, S. E.: A modeling study of the mechanism of the halogen–ozone–mercury homogeneous reactions in the troposphere during the polar spring, *Atmos. Environ.*, 37, 4467–4481, 2003.
- Carpenter, L. J. and Liss, P. S.: On temperate sources of bromoform and other reactive organic bromine gases, *J. Geophys. Res.*, 105, 20539–20547, 2000.
- Carpenter, L. J., Sturges, W. T., Penkett, S. A., Liss, P. S., Alicke, B., Hebestreit, K., and Platt, U.: Short-lived alkyl iodides and bromides at Mace Head, Ireland: Links to biogenic sources and halogen oxide production, *J. Geophys. Res.*, 104, 1679–1689, 1999.
- Carpenter, L. J., Liss, P. S., and Penkett, S. A.: Marine organohalogenes in the atmosphere over the Atlantic and Southern Oceans, *J. Geophys. Res.*, 108, 4256, doi:10.1029/2002JD002769, 2003.
- Carpenter, L. J., Wevill, D. J., Hopkins, J. R., Dunk, R. M., Jones, C. E., Hornsby, K. E., and McQuaid, J. B.: Bromoform in tropical Atlantic air from 25° N to 25 degrees S, *Geophys. Res. Lett.*, 34, L11810, doi:10.1029/2007GL029893, 2007.
- Carpenter, L. J., Jones, C. E., Dunk, R. M., Hornsby, K. E., and Woeltjen, J.: Air-sea fluxes of biogenic bromine from the tropical and North Atlantic Ocean, *Atmos. Chem. Phys.*, 9, 1805–1816, doi:10.5194/acp-9-1805-2009, 2009.
- Chuck, A. L., Turner, S. M., and Liss, P. S.: Oceanic distributions and air-sea fluxes of biogenic halocarbons in the open ocean, *J. Geophys. Res.*, 110, C10022, doi:10.1029/2004JC002741, 2005.
- Class, T. H. and Ballschmiter, K.: Chemistry of Organic Traces in Air VIII: Sources and Distribution of Bromo- and Bromochloromethanes in Marine Air and Surfacewater of the Atlantic Ocean, *J. Atmos. Chem.*, 6, 35–46, 1988.
- Dvortsov, V. L., Geller, M. A., Solomon, S., Schauffler, S. M., Atlas, E. L., and Blake, D. R.: Rethinking halogen budgets in the

- midlatitude lower stratosphere, *Geophys. Res. Lett.*, 26, 1699–1702, 1999.
- Emmons, L. K., Walters, S., Hess, P. G., Lamarque, J.-F., Pfister, G. G., Fillmore, D., Granier, C., Guenther, A., Kinnison, D., Laepple, T., Orlando, J., Tie, X., Tyndall, G., Wiedinmyer, C., Baughcum, S. L., and Kloster, S.: Description and evaluation of the Model for Ozone and Related chemical Tracers, version 4 (MOZART-4), *Geosci. Model Dev.*, 3, 43–67, doi:10.5194/gmd-3-43-2010, 2010.
- Fraser, P. J., Oram, D. E., Reeves, C. E., Penkett, S. A., and McCulloch, A.: Southern Hemispheric halon trends (1978–1998) and global halon emissions, *J. Geophys. Res.*, 104, 15985–15999, 1999.
- Gent, P. R., Yeager, S. G., Neale, R. B., Levis, S., and Bailey, D. A.: Improvements in a half degree atmosphere/land version of the CCSM, *Clim. Dynam.*, 34, 819–833, doi:10.1007/s00382-009-0614-8, 2010.
- Gent, P. R., Danabasoglu, G., Donner, L. J., Holland, M. M., Hunke, E. C., Jayne, S. R., Lawrence, D. M., Neale, R. B., Rasch, P. J., Vertenstein, M., Worley, P. H., Yang, Z.-L., and Zhang, M.: The Community Climate System Model Version 4, *J. Climate*, 24, 4973–4991, 2011.
- Giese, B., Laturmus, F., Adams, F. C., and Wiencke, C.: Release of volatile iodinated C<sub>1</sub>–C<sub>4</sub> hydrocarbons by marine macroalgae from various climate zones, *Environ. Sci. Technol.*, 33, 2432–2439, 1999.
- Hagan, D. E., Webster, C. R., Farmer, C. B., May, R. D., Herman, R. L., Weinstock, E. M., Christensen, L. E., Lait, L. R., and Newman, P. A.: Validating AIRS upper atmosphere water vapor retrievals using aircraft and balloon in situ measurements, *Geophys. Res. Lett.*, 31, L21103, doi:10.1029/2004GL020302, 2004.
- Happell, J. D. and Wallace, D. W. R.: Methyl iodide in the Greenland/Norwegian Seas and the tropical Atlantic Ocean: Evidence for photochemical production, *Geophys. Res. Lett.*, 23, 2105–2108 doi:10.1029/96GL01764, 1996.
- Hoell, J. M., Davis, D. D., Jacob, D. J., Rodgers, M. O., Newell, R. E., Fuelberg, H. E., McNeal, R. J., Raper, J. L., and Bendura, R. J.: Pacific Exploratory Mission in the tropical Pacific: PEM-Tropics A, August–September 1996, *J. Geophys. Res.*, 104, 5567–5583, 1999.
- Holmes, C. D., Jacob, D. J., Corbitt, E. S., Mao, J., Yang, X., Talbot, R., and Slemr, F.: Global atmospheric model for mercury including oxidation by bromine atoms, *Atmos. Chem. Phys.*, 10, 12037–12057, doi:10.5194/acp-10-12037-2010, 2010.
- Hossaini, R., Chipperfield, M. P., Monge-Sanz, B. M., Richards, N. A. D., Atlas, E., and Blake, D. R.: Bromoform and dibromomethane in the tropics: a 3-D model study of chemistry and transport, *Atmos. Chem. Phys.*, 10, 719–735, doi:10.5194/acp-10-719-2010, 2010.
- Hossaini, R., Chipperfield, M. P., Feng, W., Breider, T. J., Atlas, E., Montzka, S. A., Miller, B. R., Moore, F., and Elkins, J.: The contribution of natural and anthropogenic very short-lived species to stratospheric bromine, *Atmos. Chem. Phys.*, 12, 371–380, doi:10.5194/acp-12-371-2012, 2012.
- Jacob, D. J., Crawford, J. H., Kleb, M. M., Connors, V. S., Bendura, R. J., Raper, J. L., Sachse, G. W., Gille, J. C., Emmons, L., and Heald, C. L.: Transport and Chemical Evolution over the Pacific (TRACE-P) aircraft mission: Design, execution, and first results, *J. Geophys. Res.*, 108, 9000, doi:10.1029/2002JD003276, 2003.
- Jacob, D. J., Crawford, J. H., Maring, H., Clarke, A. D., Dibb, J. E., Emmons, L. K., Ferrare, R. A., Hostetler, C. A., Russell, P. B., Singh, H. B., Thompson, A. M., Shaw, G. E., McCauley, E., Pederson, J. R., and Fisher, J. A.: The Arctic Research of the Composition of the Troposphere from Aircraft and Satellites (ARCTAS) mission: design, execution, and first results, *Atmos. Chem. Phys.*, 10, 5191–5212, doi:10.5194/acp-10-5191-2010, 2010.
- Jones, C. E., Hornsby, K. E., Dunk, R. M., Leigh, R. J., and Carpenter, L. J.: Coastal measurements of short-lived reactive iodocarbons and bromocarbons at Roscoff, Brittany during the RHAMBLE campaign, *Atmos. Chem. Phys.*, 9, 8757–8769, doi:10.5194/acp-9-8757-2009, 2009.
- Jones, C. E., Hornsby, K. E., Sommariva, R., Dunk, R. M., von Glasow, R., McFiggans, G., and Carpenter, L. J.: Quantifying the contribution of marine organic gases to atmospheric iodine, *Geophys. Res. Lett.*, 37, L18804, doi:10.1029/2010GL043990, 2010.
- Kerkweg, A., Jöckel, P., Warwick, N., Gebhardt, S., Brenninkmeijer, C. A. M., and Lelieveld, J.: Consistent simulation of bromine chemistry from the marine boundary layer to the stratosphere – Part 2: Bromocarbons, *Atmos. Chem. Phys.*, 8, 5919–5939, doi:10.5194/acp-8-5919-2008, 2008.
- Kinnison, D. E., Brasseur, G. P., Walters, S., Garcia, R. R., Marsh, D. R., and Sassi, F., Harvey, V. L., Randall, C. E., Emmons, L., Lamarque, J. F., Hess, P., Orlando, J. J., Tie, X. X., Randel, W., Pan, L. L., Gettelman, A., Granier, C., Diehl, T., Niemeier, U., and Simmons, A. J.: Sensitivity of chemical tracers to meteorological parameters in the MOZART-3 chemical transport model, *J. Geophys. Res.*, 112, D20302, doi:10.1029/2006JD007879, 2007.
- Kourtidis, K., Borchers, R., and Fabian, P.: Vertical distribution of methyl bromide in the stratosphere, *Geophys. Res. Lett.*, 25, 505–508, 1998.
- Kroon, M., Petropavlovskikh, I., Shetter, R., Hall, S., Ullmann, K., Veeffkind, J. P., McPeters, R. D., Browell, E. V., and Levelt, P. F.: OMI total ozone column validation with Aura-AVE CAFS observations, *J. Geophys. Res.*, 113, D15S13, doi:10.1029/2007JD008795, 2008.
- Lamarque, J.-F. and Solomon, S.: Impact of Changes in Climate and Halocarbons on Recent Lower Stratosphere Ozone and Temperature Trends, *J. Climate*, 23, 2599–2611, 2010.
- Lamarque, J.-F., Bond, T. C., Eyring, V., Granier, C., Heil, A., Klimont, Z., Lee, D., Liouise, C., Mieville, A., Owen, B., Schultz, M. G., Shindell, D., Smith, S. J., Stehfest, E., Van Aardenne, J., Cooper, O. R., Kainuma, M., Mahowald, N., McConnell, J. R., Naik, V., Riahi, K., and van Vuuren, D. P.: Historical (1850–2000) gridded anthropogenic and biomass burning emissions of reactive gases and aerosols: methodology and application, *Atmos. Chem. Phys.*, 10, 7017–7039, doi:10.5194/acp-10-7017-2010, 2010.
- Lamarque, J.-F., Emmons, L. K., Hess, P. G., Kinnison, D. E., Tilmes, S., Vitt, F., Heald, C. L., Holland, E. A., Lauritzen, P. H., Neu, J., Orlando, J. J., Rasch, P., and Tyndall, G.: CAM-chem: description and evaluation of interactive atmospheric chemistry in CESM, *Geosci. Model Dev. Discuss.*, 4, 2199–2278, doi:10.5194/gmdd-4-2199-2011, 2011.
- Lawrence, M. G., Jöckel, P., and von Kuhlmann, R.: What does the global mean OH concentration tell us?, *Atmos. Chem. Phys.*, 1,

- 37–49, doi:10.5194/acp-1-37-2001, 2001.
- Lee, J. D., McFiggans, G., Allan, J. D., Baker, A. R., Ball, S. M., Benton, A. K., Carpenter, L. J., Commane, R., Finley, B. D., Evans, M., Fuentes, E., Furneaux, K., Goddard, A., Good, N., Hamilton, J. F., Heard, D. E., Herrmann, H., Hollingsworth, A., Hopkins, J. R., Ingham, T., Irwin, M., Jones, C. E., Jones, R. L., Keene, W. C., Lawler, M. J., Lehmann, S., Lewis, A. C., Long, M. S., Mahajan, A., Methven, J., Moller, S. J., Müller, K., Müller, T., Niedermeier, N., O'Doherty, S., Oetjen, H., Plane, J. M. C., Pszenny, A. A. P., Read, K. A., Saiz-Lopez, A., Saltzman, E. S., Sander, R., von Glasow, R., Whalley, L., Wiedensohler, A., and Young, D.: Reactive Halogens in the Marine Boundary Layer (RHAMBLE): the tropical North Atlantic experiments, *Atmos. Chem. Phys.*, 10, 1031–1055, doi:10.5194/acp-10-1031-2010, 2010.
- Liang, Q., Stolarski, R. S., Kawa, S. R., Nielsen, J. E., Douglass, A. R., Rodriguez, J. M., Blake, D. R., Atlas, E. L., and Ott, L. E.: Finding the missing stratospheric Br<sub>y</sub>: a global modeling study of CHBr<sub>3</sub> and CH<sub>2</sub>Br<sub>2</sub>, *Atmos. Chem. Phys.*, 10, 2269–2286, doi:10.5194/acp-10-2269-2010, 2010.
- Liao, H., Adams, P. J., Chung, S. H., Seinfeld, J. H., Mickley, L. J., and Jacob, D. J.: Interactions between tropospheric chemistry and aerosols in a unified general circulation model, *J. Geophys. Res.*, 108, 4001, doi:10.1029/2001JD001260, 2003.
- Mahowald, N. M., Lamarque, J.-F., Tie, X. X., and Wolff, E.: Sea-salt aerosol response to climate change: Last Glacial Maximum, preindustrial, and doubled carbon dioxide climates, *J. Geophys. Res.*, 111, D05303, doi:10.1029/2005JD006459, 2006a.
- Mahowald, N. M., Muhs, D. R., Levis, S., Rasch, P. J., Yoshioka, M., Zender, C. S., and Luo, C.: Change in atmospheric mineral aerosols in response to climate: Last glacial period, preindustrial, modern, and doubled carbon dioxide climates, *J. Geophys. Res.*, 111, D10202, doi:10.1029/2005JD006653, 2006b.
- Martino, M., Mills, G. P., Woeltjen, J., and Liss, P. S.: A new source of volatile organoiodine compounds in surface seawater, *Geophys. Res. Lett.*, 36, L01609, doi:10.1029/2008GL036334, 2009.
- Mellouki, A., Talukdar, R. K., Schmoltnner, A.-M., Gierczak, T., Mills, M. J., Solomon, S., and Ravishankara, A. R.: Atmospheric lifetimes and ozone depletion potentials of methyl bromide (CH<sub>3</sub>Br) and dibromomethane (CH<sub>2</sub>Br<sub>2</sub>), *Geophys. Res. Lett.*, 19, 2059–2062, 1992.
- Metzger, S., Dentener, F., Pandis, S., and Lelieveld, J.: Gas/aerosol partitioning: 1. A computationally efficient model, *J. Geophys. Res.*, 107, 4312, doi:10.1029/2001JD001102, 2002.
- Moore, R. and Tokarczyk, R.: Volatile Biogenic Halocarbons in the Northwest Atlantic, *Global Biogeochem. Cy.*, 7, 195–210, 1993.
- Moore, R. and Zafiriou, O.: Photochemical production of methyl iodide in seawater, *J. Geophys. Res.*, 99, 16415–16420, doi:10.1029/94JD00786, 1994.
- Moore, R., Webb, M., Tokarczyk, R., and Wever, R.: Bromoperoxidase and iodoperoxidase enzymes and production of halogenated methanes in marine diatom cultures, *J. Geophys. Res.*, 101, 20899–20908, 1996.
- Neale, R. B., Richter, J. H., and Jochum, M.: The impact of convection on ENSO: From a delayed oscillator to a series of events, *J. Climate*, 21, 5904–5924, 2008.
- Newman, P. A., Fahey, D. W., Brune, W. H., Kurylo, M. J., and Kawa, S. R.: Preface – Photochemistry of Ozone Loss in the Arctic Region in Summer (POLARIS), *J. Geophys. Res.*, 104, 26481–26495, 1999.
- Newman, P. A., Harris, N. R. P., Adriani, A., Amanatidis, G. T., Anderson, J. G., Braathen, G. O., Brune, W. H., Carslaw, K. S., Craig, M. S., DeCola, P. L., Guirlet, M., Hipskind, R. S., Kurylo, M. J., Küllmann, H., Larsen, N., Mégie, G. J., Pommereau, J.-P., Poole, L. R., Schoeberl, M. R., Strohm, F., Toon, O. B., Trepte, C. R., and Van Roozendael, M.: An overview of the SOLVE/THESEO 2000 campaign, *J. Geophys. Res.*, 107, 8259, doi:10.1029/2001JD001303, 2002.
- Obrist, D., Tas, E., Peleg, M., Matveev, V., Faïn, X., Asaf, D., and Luria, M.: Bromine-induced oxidation of mercury in the mid-latitude atmosphere, *Nat. Geosci.*, 4, 22–26, 2011.
- Peters, C., Pechtl, S., Stutz, J., Hebestreit, K., Hönninger, G., Heumann, K. G., Schwarz, A., Winterlik, J., and Platt, U.: Reactive and organic halogen species in three different European coastal environments, *Atmos. Chem. Phys.*, 5, 3357–3375, doi:10.5194/acp-5-3357-2005, 2005.
- Pfister, L., Selkirk, H. B., Starr, D. O., Rosenlof, K., and Newman, P. A.: A meteorological overview of the TC4 mission, *J. Geophys. Res.*, 115, D00J12, doi:10.1029/2009JD013316, 2010.
- Quack, B. and Wallace, D. W. R.: Air-sea flux of bromoform: Controls, rates, and implications, *Global Biogeochem. Cy.*, 17, 1023, doi:10.1029/2002GB001890, 2003.
- Raper, J. L., Kleb, M. M., Jacob, D. J., Davis, D. D., Newell, R. E., Fuelberg, H. E., Bendura, R. J., Hoell, J. M., and McNeal, R. J.: Pacific Exploratory Mission in the Tropical Pacific: PEM-Tropics B, March–April 1999, *J. Geophys. Res.*, 106, 32401–32425, 2001.
- Rayner, N. A., Parker, D. E., Horton, E. B., Folland, C. K., Alexander, L. V., Rowell, D. P., Kent, E. C., and Kaplan, A.: Global analyses of sea surface temperature, sea ice, and night marine air temperature since the late nineteenth century, *J. Geophys. Res.*, 108, 4407, doi:10.1029/2002JD002670, 2003.
- Read, K. A., Mahajan, A. S., Carpenter, L. J., Evans, M. J., Faria, B. V. E., Heard, D. E., Hopkins, J. R., Lee, J. D., Moller, S. J., Lewis, A. C., Mendes, L., McQuaid, J. B., Oetjen, H., Saiz-Lopez, A., Pilling, M. J., and Plane, J. M. C.: Extensive halogen-mediated ozone destruction over the tropical Atlantic Ocean, *Nature*, 453, 1232–1235, 2008.
- Richter, J. H. and Rasch, P. J.: Effects of convective momentum transport on the atmospheric circulation in the Community Atmosphere Model, version 3, *J. Climate*, 21, 1487–1499, 2008.
- Roehl, C. M., Burkholder, J. B., Moortgat, G. K., Ravishankara, A. R., and Crutzen, P. J.: Temperature dependence of UV absorption cross sections and atmospheric implications of several alkyl iodides, *J. Geophys. Res.*, 102, 12819–12829, 1997.
- Saiz-Lopez, A., Mahajan, A. S., Salmon, R. A., Bauguitte, S. J.-B., Jones, A. E., Roscoe, H. K., and Plane, J. M. C.: Boundary Layer Halogens in Coastal Antarctica, *Science*, 317, 348–351, 2007.
- Saiz-Lopez, A., Plane, J. M. C., Mahajan, A. S., Anderson, P. S., Bauguitte, S. J.-B., Jones, A. E., Roscoe, H. K., Salmon, R. A., Bloss, W. J., Lee, J. D., and Heard, D. E.: On the vertical distribution of boundary layer halogens over coastal Antarctica: implications for O<sub>3</sub>, HO<sub>x</sub>, NO<sub>x</sub> and the Hg lifetime, *Atmos. Chem. Phys.*, 8, 887–900, doi:10.5194/acp-8-887-2008, 2008.
- Saiz-Lopez, A., Lamarque, J.-F., Kinnison, D. E., Tilmes, S., Ordóñez, C., Orlando, J. J., Conley, A. J., Plane, J. M. C., Mahajan, A. S., Sousa Santos, G., Atlas, E. L., Blake, D. R., Sander, S. P., Schauffler, S., Thompson, A. M., and Brasseur, G.: Estim-

- ing the climate significance of halogen-driven ozone loss in the tropical marine troposphere, *Atmos. Chem. Phys. Discuss.*, 11, 32003–32029, doi:10.5194/acpd-11-32003-2011, 2011.
- Salawitch, R. J., Weisenstein, D. K., Kovalenko, L. J., Sioris, C. E., Wennberg, P. O., Chance, K., Ko, M. K. W., and McLinden, C. A.: Sensitivity of ozone to bromine in the lower stratosphere, *Geophys. Res. Lett.*, 32, L05811, doi:10.1029/2004GL021504, 2005.
- Sander, R., Keene, W. C., Pszenny, A. A. P., Arimoto, R., Ayers, G. P., Baboukas, E., Cainey, J. M., Crutzen, P. J., Duce, R. A., Hönninger, G., Huebert, B. J., Maenhaut, W., Mihalopoulos, N., Turekian, V. C., and Van Dingenen, R.: Inorganic bromine in the marine boundary layer: a critical review, *Atmos. Chem. Phys.*, 3, 1301–1336, doi:10.5194/acp-3-1301-2003, 2003a.
- Sander, S. P., Friedl, R. R., Golden, D. M., Kurylo, M. J., Huie, R. E., Orkin, V. L., Moortgat, G. K., Ravishankara, A. R., Kolb, C. E., Molina, M. J., and Finlayson-Pitts, B. J.: Chemical Kinetics and Photochemical Data for Use in Atmospheric Studies – Evaluation Number 14, JPL Publication 02-25, 2003b.
- Sander, S. P., Friedl, R. R., Golden, D. M., Kurylo, M. J., Moortgat, G. K., Keller-Rudek, H., Wine, P. H., Ravishankara, A. R., Kolb, C. E., Molina, M. J., Finlayson-Pitts, B. J., Huie, R. E., and Orkin, V. L.: Chemical Kinetics and Photochemical Data for Use in Atmospheric Studies – Evaluation Number 15, JPL Publication 06-2, 2006.
- Schauffler, S. M., Heidt, L. E., Pollock, W. H., Gilpin, T. M., Veder, J. F., Solomon, S., Lueb, R. A., and Atlas, E. L.: Measurements of halogenated organic compounds near the tropical tropopause, *Geophys. Res. Lett.*, 20, 2567–2570, 1993.
- Schauffler, S. M., Atlas, E. L., Blake, D. R., Flocke, F., Lueb, R. A., Lee-Taylor, J. M., Stroud, V., and Travnicek, W.: Distributions of brominated organic compounds in the troposphere and lower stratosphere, *J. Geophys. Res.*, 104, 21513–21535, 1999.
- Schofield, R., Fueglistaler, S., Wohltmann, I., and Rex, M.: Sensitivity of stratospheric Br<sub>2</sub> to uncertainties in very short lived substance emissions and atmospheric transport, *Atmos. Chem. Phys.*, 11, 1379–1392, doi:10.5194/acp-11-1379-2011, 2011.
- Schroeder, W. H., Anlauf, K. G., Barrie, L. A., Lu, J. Y., Steffen, A., Schneeberger, D. R., and Berg, T.: Arctic springtime depletion of mercury, *Nature*, 394, 331–332, 1998.
- Singh, H. B., Brune, W. H., Crawford, J. H., Jacob, D. J., and Russell, P. B.: Overview of the summer 2004 Intercontinental Chemical Transport Experiment-North America (INTEX-A), *J. Geophys. Res.*, 111, D24S01, doi:10.1029/2006JD007905, 2006.
- Singh, H. B., Brune, W. H., Crawford, J. H., Flocke, F., and Jacob, D. J.: Chemistry and transport of pollution over the Gulf of Mexico and the Pacific: spring 2006 INTEX-B campaign overview and first results, *Atmos. Chem. Phys.*, 9, 2301–2318, doi:10.5194/acp-9-2301-2009, 2009.
- Solomon, S., Garcia, R. R., and Ravishankara, A. R.: On the role of iodine in ozone depletion, *J. Geophys. Res.*, 99, 20491–20499, 1994.
- Sousa Santos, G.: The Effect of Halogens on Global Tropospheric Ozone, PhD Thesis, Max Planck Institute for Meteorology, Hamburg, Germany, 2008.
- Sturges, W. T., Cota, G. F., and Buckley, P. T.: Bromoform emission from Arctic ice algae, *Nature*, 358, 660–662, 1992.
- Sturges, W. T., Cota, G. F., and Buckley, P. T.: Vertical profiles of bromoform in snow, sea ice, and seawater in the Canadian Arctic, *J. Geophys. Res.*, 102, 25073–25083, 1997.
- Tie, X., Brasseur, G., Emmons, L., Horowitz, L., and Kinnison, D.: Effects of aerosols on tropospheric oxidants: A global model study, *J. Geophys. Res.*, 106, 22931–22964, 2001.
- Tie, X., Madronich, S., Walters, S., Edwards, D. P., Ginoux, P., Mahowald, N., Zhang, R., Lou, C., and Brasseur, G.: Assessment of the global impact of aerosols on tropospheric oxidants, *J. Geophys. Res.*, 110, D03204, doi:10.1029/2004JD005359, 2005.
- Toon, O. B., Starr, D. O., Jensen, E. J., Newman, P. A., Platnick, S., Schoeberl, M. R., Wennberg, P. O., Wofsy, S. C., Kurylo, M. J., Maring, H., Jucks, K. W., Craig, M. S., Vasques, M. F., Pfister, L., Rosenlof, K. H., Selkirk, H. B., Colarco, P. R., Kawa, S. R., Mace, G. G., Minnis, P., and Pickering, K. E.: Planning, implementation, and first results of the Tropical Composition, Cloud and Climate Coupling Experiment (TC4), *J. Geophys. Res.*, 115, D00J04, doi:10.1029/2009JD013073, 2010.
- Varner, R. K., Zhou, Y., Russo, R. S., Wingenter, O. W., Atlas, E., Stroud, C., Mao, H., Talbot, R., and Sive, B. C.: Controls on atmospheric chloroiodomethane (CH<sub>2</sub>CI) in marine environments, *J. Geophys. Res.*, 113, D10303, doi:10.1029/2007JD008889, 2008.
- Vogt, R., Crutzen, P. J., and Sander, R.: A mechanism for halogen release from sea-salt aerosol in the remote marine boundary layer, *Nature*, 383, 327–330, 1996.
- von Glasow, R. and Crutzen, P. J.: Tropospheric Halogen Chemistry, in: *Treatise on Geochemistry*, edited by: Holland, H. D. and Turekian, K. K., Elsevier Ltd., ISBN: 0-08-043751-6, 67 pp., 2007.
- Wamsley, P. R., Elkins, J. W., Fahey, D. W., Dutton, G. S., Volk, C. M., Myers, R. C., Montzka, S. A., Butler, J. H., Clarkel, A. D., Fraser, P. J., Steele, L. P., Lucarelli, M. P., Atlas, E. L., Schauffler, S. M., Blake, D. R., Rowland, F. S., Sturges, W. T., Lee, J. M., Penkett, S. A., Engel, A., Stimpfle, R. M., Chan, K. R., Weisenstein, D. K., Ko, M. K. W., and Salawitch, R. J.: Distribution of halon-1211 in the upper troposphere and lower stratosphere and the 1994 total bromine budget, *J. Geophys. Res.*, 103, 1513–1526, 1998.
- Warwick, N. J., Pyle, J. A., Carver, G. D., Yang, X., Savage, N. H., O'Connor, F. M., and Cox, R. A.: Global modelling of biogenic bromocarbons, *J. Geophys. Res.*, 111, D24305, doi:10.1029/2006JD007264, 2006a.
- Warwick, N. J., Pyle, J. A., and Shallcross, D. E.: Global Modelling of the Atmospheric Methyl Bromide Budget, *J. Atmos. Chem.*, 54, 133–159, 2006b.
- Wofsy, S. C., the HIPPO Science Team, and Cooperating Modelers and Satellite Teams: HIAPER Pole-to-Pole Observations (HIPPO): fine-grained, global-scale measurements of climatically important atmospheric gases and aerosols, *Philos. T. Roy. Soc. A*, 369, 2073–2086, 2011.
- World Meteorological Organization (WMO): Scientific Assessment of Ozone Depletion: 2002, Global Ozone Research and Monitoring Project-Report No. 47, 498 pp., Geneva, Switzerland, 2003.
- World Meteorological Organization (WMO): Scientific Assessment of Ozone Depletion: 2006, Global Ozone Research and Monitoring Project-Report No. 50, 572 pp., Geneva, Switzerland, 2007.
- World Meteorological Organization (WMO): Scientific Assessment of Ozone Depletion: 2010, Global Ozone Research and Monitoring Project-Report No. 52, 516 pp., Geneva, Switzerland, 2011.
- Yamamoto, H., Yokouchi, Y., Otsuki, A., and Itoh, H.: Depth pro-

- files of volatile halogenated hydrocarbons in seawater in the Bay of Bengal, *Chemosphere*, 45, 371–377, 2001.
- Yang, X., Cox, R. A., Warwick, N. J., Pyle, J. A., Carver, G. D., O'Connor, F. M., and Savage, N. H.: Tropospheric bromine chemistry and its impacts on ozone: A model study, *J. Geophys. Res.*, 110, D23311, doi:10.1029/2005JD006244, 2005.
- Yokouchi, Y., Hasebe, F., Fujiwara, M., Takashima, H., Shiotani, M., Nishi, N., Kanaya, Y., Hashimoto, S., Fraser, P., Toom-Sauntry, D., Mukai, H., and Nojiri, Y.: Correlations and emission ratios among bromoform, dibromochloromethane, and dibromomethane in the atmosphere, *J. Geophys. Res.*, 110, D23309, doi:10.1029/2005JD006303, 2005.
- Yokouchi, Y., Osada, K., Wada, M., Hasebe, F., Agama, M., Murakami, R., Mukai, H., Nojiri, Y., Inuzuka, Y., Toom-Sauntry, D., and Fraser, P.: Global distribution and seasonal concentration change of methyl iodide in the atmosphere, *J. Geophys. Res.*, 113, D18311, doi:10.1029/2008JD009861, 2008.
- Yokouchi, Y., Saito, T., Ooki, A., and Mukai, H.: Diurnal and seasonal variations of iodocarbons ( $\text{CH}_2\text{ClI}$ ,  $\text{CH}_2\text{I}_2$ ,  $\text{CH}_3\text{I}$ , and  $\text{C}_2\text{H}_5\text{I}$ ) in the marine atmosphere, *J. Geophys. Res.*, 116, D06301, doi:10.1029/2010JD015252, 2011.
- Youn, D., Patten, K. O., Wuebbles, D. J., Lee, H., and So, C.-W.: Potential impact of iodinated replacement compounds  $\text{CF}_3\text{I}$  and  $\text{CH}_3\text{I}$  on atmospheric ozone: a three-dimensional modeling study, *Atmos. Chem. Phys.*, 10, 10129–10144, doi:10.5194/acp-10-10129-2010, 2010.
- Yvon-Lewis, S. A. and Butler, J. H.: The potential effect of oceanic biological degradation on the lifetime of atmospheric  $\text{CH}_3\text{Br}$ , *Geophys. Res. Lett.*, 24, 1227–1230, 1997.
- Zhang, G. J. and McFarlane, N. A.: Sensitivity of climate simulations to the parameterization of cumulus convection in the Canadian Climate Centre general circulation model, *Atmos. Ocean*, 33, 407–446, 1995.